Title

Persistent behavior deficits, neuroinflammation, and oxidative stress in a rat model of acute organophosphate intoxication

Authors

Guignet, Michelle
Dhakal, Kiran
Flannery, Brenna M
et al.

Publication Date

2020

DOI

10.1016/j.nbd.2019.03.019

Peer reviewed

Neurobiology of Disease xxx (xxxx) xxx–xxx

Contents lists available at ScienceDirect

Neurobiology of Disease

journal homepage: www.elsevier.com/locate/ynbdi

Review

Persistent behavior deficits, neuroinflammation, and oxidative stress in a rat model of acute organophosphate intoxication

Michelle Guignet[a,1], Kiran Dhakal[a,1], Brenna M. Flannery[a], Brad A. Hobson[a], Dorota Zolkowska[b], Ashish Dhir[b], Donald A. Bruun[a], Shuyang Li[c], Abdul Wahab[b], Danielle J. Harvey[c], Jill L. Silverman[d,e], Michael A. Rogawski[b], Pamela J. Lein[a,e,*]

[a] Department of Molecular Biosciences, School of Veterinary Medicine, University of California-Davis, 1089 Veterinary Medicine Drive, Davis, CA 95616, USA
[b] Department of Neurology, School of Medicine, University of California-Davis, 4860 Y Street, Sacramento, CA 95817, USA
[c] Department of Public Health Sciences, University of California-Davis, One Shields Avenue, Davis, CA 95616, USA
[d] Department of Psychiatry and Behavioral Sciences, School of Medicine, University of California-Davis, 2230 Stockton Boulevard, Sacramento, CA 95817, USA
[e] MIND Institute, School of Medicine, University of California-Davis, 2825 50th Street, Sacramento, CA 95817, USA

ARTICLE INFO

Keywords:
Behavior
Cognition
Diisopropylfluorophosphate
Electroencephalography
Microgliosis
Persistent effects
Preclinical model
Reactive astrogliosis
Spontaneous recurrent seizures
Sublethal toxicity

ABSTRACT

Current medical countermeasures for organophosphate (OP)-induced *status epilepticus* (SE) are not effective in preventing long-term morbidity and there is an urgent need for improved therapies. Rat models of acute intoxication with the OP, diisopropylfluorophosphate (DFP), are increasingly being used to evaluate therapeutic candidates for efficacy in mitigating the long-term neurologic effects associated with OP-induced SE. Many of these therapeutic candidates target neuroinflammation and oxidative stress because of their implication in the pathogenesis of persistent neurologic deficits associated with OP-induced SE. Critical to these efforts is the rigorous characterization of the rat DFP model with respect to outcomes associated with acute OP intoxication in humans, which include long-term electroencephalographic, neurobehavioral, and neuropathologic effects, and their temporal relationship to neuroinflammation and oxidative stress. To address these needs, we examined a range of outcomes at later times post-exposure than have previously been reported for this model. Adult male Sprague-Dawley rats were given pyridostigmine bromide (0.1 mg/kg, im) 30 min prior to administration of DFP (4 mg/kg, sc), which was immediately followed by atropine sulfate (2 mg/kg, im) and pralidoxime (25 mg/kg, im). This exposure paradigm triggered robust electroencephalographic and behavioral seizures that rapidly progressed to SE lasting several hours in 90% of exposed animals. Animals that survived DFP-induced SE (~70%) exhibited spontaneous recurrent seizures and hyperreactive responses to tactile stimuli over the first 2 months post-exposure. Performance in the elevated plus maze, open field, and Pavlovian fear conditioning tests indicated that acute DFP intoxication reduced anxiety-like behavior and impaired learning and memory at 1 and 2 months post-exposure in the absence of effects on general locomotor behavior. Immunohistochemical analyses revealed significantly increased expression of biomarkers of reactive astrogliosis, microglial activation and oxidative stress in multiple brain regions at 1 and 2 months post-DFP, although there was significant spatiotemporal heterogeneity across these endpoints. Collectively, these data largely support the relevance of the rat model of acute DFP intoxication as a model for acute OP intoxication in the human, and support the hypothesis that neuroinflammation and/or oxidative stress represent potential therapeutic targets for mitigating the long-term neurologic sequelae of acute OP intoxication.

Abbreviations: CounterACT, Countermeasures Against Chemical Threats program; DFP, diisopropylfluorophosphate; EEG, electroencephalography; EPM, elevated plus maze; GFAP, glial fibrillary acidic protein; IBA-1, ionized calcium binding adaptor molecule 1; NIH, National Institutes of Health; 3-NT, 3-nitrotyrosine; OP, organophosphate; 2-PAM, 2-pralidoxime; PBS, phosphate-buffered saline; PET, positron emission tomography; SD, standard deviation; SE, *status epilepticus*; SEM, standard error of the mean; SRS, spontaneous recurrent seizures; TSPO, 18 kD mitochondrial membrane translocator protein; VEH, vehicle

* Corresponding author at: Department of Molecular Biosciences, School of Veterinary Medicine, University of California-Davis, 1089 Veterinary Medicine Drive, Davis, CA 95616, USA.

E-mail addresses: mguignet@ucdavis.edu (M. Guignet), bahobson@ucdavis.edu (B.A. Hobson), dzolkowska@ucdavis.edu (D. Zolkowska), dhir@ucdavis.edu (A. Dhir), dabruun@ucdavis.edu (D.A. Bruun), shyli@ucdavis.edu (S. Li), djharvey@ucdavis.edu (D.J. Harvey), jsilverman@ucdavis.edu (J.L. Silverman), rogawski@ucdavis.edu (M.A. Rogawski), pjlein@ucdavis.edu (P.J. Lein).

[1] These authors contributed equally to this work.

https://doi.org/10.1016/j.nbd.2019.03.019
Received 22 December 2018; Received in revised form 5 March 2019; Accepted 20 March 2019

1. Introduction

Acute intoxication with organophosphate (OP) cholinesterase inhibitors is a significant public health concern. OP warfare agents continue to be used as weapons of war and terrorism, as exemplified by the 2013 and 2017 chemical attacks in Syria (UN, 2017; Vogel, 2013), the 2017 assassination of Korean leader Kim Jong-un's half-brother (OPCW, 2017), and the 2018 poisoning of a former Russian spy and his daughter in Great Britain (Haley, 2018). Acute intoxication with OP pesticides is estimated to cause > 3 million life-threatening human poisonings each year, and over 250,000 deaths from self-poisoning, the latter accounting for about one-third of the world's suicide cases (Gunnell et al., 2007; Mew et al., 2017; Pereira et al., 2014).

The canonical mechanism of action of acute OP neurotoxicity is inhibition of acetylcholinesterase, which triggers both peripheral and central cholinergic effects that collectively define a clinical toxidrome known as cholinergic crisis (Eddleston et al., 2008; Hulse et al., 2014). Cholinergic crisis is characterized by muscle fasciculation followed by flaccid paralysis, parasympathomimetic signs, centrally mediated seizures that can quickly progress to *status epilepticus* (SE), and respiratory failure. This toxidrome is frequently fatal unless rapidly treated with atropine to block muscarinic receptors, oxime to reactivate acetylcholinesterase, and benzodiazepines to reduce seizure activity (Bird et al., 2003; Eddleston et al., 2008). Even with prompt treatment, survivors of cholinergic crisis often face significant long-term morbidity, including cognitive dysfunction, affective disorders, and electroencephalographic (EEG) abnormalities (Chen, 2012; de Araujo et al., 2012; Pereira et al., 2014). The mechanism(s) underlying the persistent neurologic effects of acute OP intoxication are not well understood, but neuroinflammation (Collombet, 2011; de Araujo et al., 2012; Guignet and Lein, 2018) and oxidative stress (Pearson and Patel, 2016; Vanova et al., 2018) are widely posited to be key pathogenic processes.

Historically, military laboratories have conducted much of the research addressing the urgent need for improved medical countermeasures for acute OP intoxication using preclinical models of SE induced by OP warfare agents. With the establishment of the National Institutes of Health (NIH) Countermeasures Against Chemical Threats (CounterACT) program (Jett and Spriggs, 2018), increasing numbers of laboratories outside the military are engaged in this area of research. This has resulted in significantly increased use of preclinical models of acute intoxication induced by OP pesticides that elicit acute neurotoxic effects similar to those of OP warfare agents, but are more readily accessible for research use. Arguably, the most widely used OP pesticide in this context is diisopropylfluorophosphate (DFP). DFP is itself considered a credible terrorist threat agent (Jett and Spriggs, 2018), in part because of its similarity in structure and toxicity to the OP warfare agents, soman and sarin (Sogorb et al., 2015). Although all seizure-inducing OPs are potent cholinesterase inhibitors, each elicits a unique profile of toxic effects (Costa, 2006; Pope, 1999; Rosenbaum and Bird, 2010). Moreover, there is evidence that inflammatory responses vary between OP nerve agents and OP pesticides (Damodaran and Abou-Donia, 2000; Grauer et al., 2008; Guignet and Lein, 2018; Liu et al., 2012), and current therapeutic strategies are not equally effective against different OPs (Eddleston et al., 2008; Rosenbaum and Bird, 2010). Thus, detailed characterization of the rat model of acute DFP intoxication is critical for identifying robust, quantifiable outcomes of human relevance for testing therapeutic candidates.

Numerous laboratories have demonstrated that the acute neurotoxic effects observed in preclinical models of acute intoxication with OP warfare agents (de Araujo et al., 2012; Pereira et al., 2014) are largely recapitulated in rat models of acute DFP intoxication. These acute effects include rapid and profound inhibition of brain and peripheral acetylcholinesterase, electroencephalographic and behavioral seizures progressing to SE that is sustained for hours, and robust neuroinflammatory responses, increased expression of oxidative stress biomarkers and extensive neurodegeneration in multiple brain regions during the first 72 h after seizure initiation (Deshpande et al., 2010; Hobson et al., 2017; Kim et al., 1999; Li et al., 2011; Liang et al., 2018; Pouliot et al., 2016; Rojas et al., 2015; Siso et al., 2017; Wu et al., 2018). However, effects at weeks to months post-exposure have not been as extensively characterized in the rat model of acute DFP intoxication. We previously demonstrated that rats acutely intoxicated with DFP exhibit learning and memory deficits at 3 weeks post-exposure in the Pavlovian fear conditioning task (Flannery et al., 2016). Other laboratories have reported cognitive impairment at 4 weeks post-exposure in the Morris water maze (Brewer et al., 2013) and at 6 to 12 weeks post-exposure in the novel object recognition task (Rojas et al., 2016). DFP-intoxicated rats are also reported to exhibit higher scores on depression-relevant immobility behavior at 8 and 29 days post-exposure (Wright et al., 2010). We have also conducted several studies examining neuropathologic outcomes in the DFP rat at times beyond 72 h post-exposure. Our initial study (Flannery et al., 2016) focused on the hippocampus and cortex using FluoroJade B staining to detect neurodegeneration and glial fibrillary acidic protein (GFAP) and ionized calcium binding adaptor molecule 1 (IBA-1) immunohistochemical analyses to quantify reactive astrogliosis and microgliosis, respectively. Neuroinflammation was also measured using positron emission tomography (PET) imaging of [^{11}C]-(*R*)-PK11195, a ligand for the 18 kD mitochondrial membrane translocator protein (TSPO), expression of which is upregulated on activated microglia and astrocytes (Guilarte, 2019). Acute DFP intoxication caused widespread neurodegeneration in the hippocampus and cortex from 1 to 14 days post-exposure, while increased neuroinflammation was detected from 1 to 21 days post-exposure (Flannery et al., 2016). A subsequent more comprehensive histological analyses of brains from rats that survived DFP-induced SE (Siso et al., 2017) revealed progressive neuronal cell death, neuroinflammation, and tissue remodeling across limbic brain regions and the cerebral cortex, with no detectable pathology in the cerebellum. While the lesion type and progression varied by time post-exposure and brain region, in general, neuronal necrosis peaked after the first week post-exposure, and neuroinflammation persisted at least 2 months after intoxication. However, to date, there are no data documenting long-term effects of acute DFP intoxication on EEG or oxidative stress in the rat brain. Moreover, these outcomes have yet to be analyzed in the same animals assessed for neurobehavioral outcomes.

Therefore, the major goal of this study was to address these data gaps by conducting a more comprehensive analysis of functional deficits and neuropathologic consequences in the DFP rat during the 2 months following DFP-induced SE. The results of this study are important for informing the design of experiments using the rat model of acute DFP intoxication to evaluate the efficacy of anti-seizure therapeutics in terminating seizures and mitigating the long-term neurologic effects associated with OP-induced SE. Additionally, the findings from this study have implications for nascent efforts to develop neuroprotective strategies that target neuroinflammation and oxidative stress (Jett and Spriggs, 2018).

2. Materials and methods

2.1. Animals and DFP exposure paradigm

All experiments involving animals complied with the ARRIVE guidelines and were performed in accordance with the National Institutes of Health guide for the care and use of laboratory animals (NIH publication No. 8023, revised 1978) following protocols approved by the University of California-Davis Institutional Animal Care and Use Committee. Adult male Sprague Dawley rats (8 ± 1 weeks old, 225–250 g, Charles River Laboratories, Hollister, CA) were individually housed in standard plastic shoebox cages in facilities fully accredited by AAALAC International under controlled environmental conditions (22 ± 2 °C, 40–50% humidity, and a 12 h light-dark cycle). Food and water were provided ad libitum. Separate cohorts of rats were used to

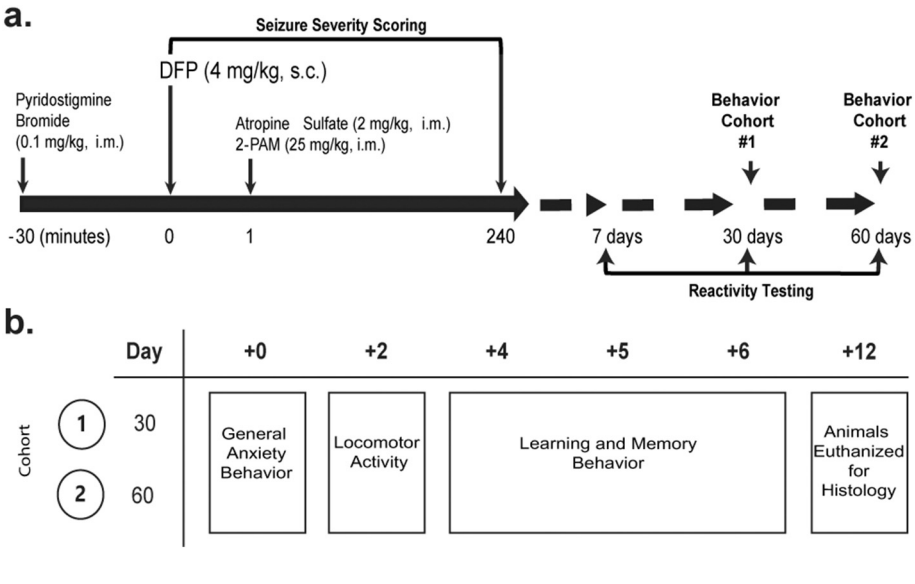

Fig. 1. Schematic illustrating the experimental model and study design. (a) Adult male Sprague Dawley rats were pretreated with pyridostigmine bromide (0.1 mg/kg, i.m.) administered 30 min prior to injection of DFP (4 mg/kg, s.c.) or equivalent volume of vehicle (PBS), followed 1 min later by a combined injection of atropine sulfate (2 mg/kg, i.m.) and 2-PAM (25 mg/kg, i.m.). All animals were assessed for reactivity to tactile stimuli at 7, 30 and 60 days post-exposure. Additional behavioral endpoints were assessed at 30 and 60 days post-exposure using separate cohorts at each time point. (b) The order of behavioral tasks assessed at 30 and 60 days post-exposure. To minimize carryover effects, behavioral tasks were performed in the order of least stressful to most stressful in all cohorts. General anxiety-like behavior was assessed using the elevated plus maze; general exploratory and locomotor behavior, the open field test; and learning and memory function, Pavlovian fear conditioning. Upon conclusion of behavior testing, all animals were euthanized, perfused and brains collected for neuropathologic analyses.

assess behavior at 1 month and 2 months post-exposure (Fig. 1). A third cohort was used to examine reactive behavior at 1 week, 1 month and 2 months following acute DFP intoxication. All behavioral studies were replicated using two separate cohorts at each time point to confirm findings.

DFP was purchased from Sigma-Aldrich (St. Louis, MO, USA), and prior to use was confirmed to be ~90 ± 7% pure as determined using previously published ^{1}H-, ^{13}C, ^{19}F and ^{31}P NMR methods (Gao et al., 2016). Upon opening a sealed vial, DFP was aliquoted and stored at −80 °C; under these conditions, it has been shown that DFP is stable for at least 400 days (Heiss et al., 2016). At the beginning of each exposure day (~8:00 AM), rats were randomly divided into either DFP or vehicle (VEH) groups using a random number generator. All animals were pretreated with 0.1 mg/kg pyridostigmine bromide (TCI America, Portland, OR, USA) in sterile isotonic saline (i.m.) 30 min prior to injection of either DFP or VEH. DFP was prepared in sterile, ice-cold phosphate buffered saline (PBS, 3.6 mM Na_2HPO_4, 1.4 mM NaH_2PO_4, 150 mM NaCl, pH 7.2) within 5 min of administration at 4 mg/kg, s.c. VEH animals received an equivalent volume (300 µl) of sterile PBS. Atropine sulfate (2 mg/kg, Sigma-Aldrich) and 2-pralidoxime (2-PAM, 25 mg/kg, Sigma-Aldrich) in sterile saline were given in a combined i.m. injection 1 min following injection of DFP to prevent lethality from peripheral cholinergic symptoms (Li et al., 2011). VEH animals were similarly injected with atropine sulfate and 2-PAM. Seizure behavior was continuously monitored for 4 h after DFP injection and scored as previously described (Siso et al., 2017). At the end of the 4 h exposure period, all DFP animals were administered 10 ml of 5% dextrose in sterile saline (s.c., Baxter Healthcare Co., Deerfield, IL, USA), returned to their home cages and given soft chow until they resumed normal consumption of water and solid food (Pessah et al., 2016).

2.2. Electroencephalographic recordings

A cohort of animals (n = 6) not used for behavioral studies was implanted with electrodes to monitor electric activity in the brain following acute DFP intoxication. Animals were anesthetized using ketamine (60 mg/kg, i.p.) and dexmedetomidine (0.5 mg/kg, i.p.) and then stabilized in a stereotaxic apparatus (Kopf Instruments, Tujunga, CA, USA). Six recording screws were implanted epidurally, three on each side of the sagittal skull suture. A 6-pin rat implant (Pinnacle 8239-SE3, Pinnacle Technology, Lawrence, KS, USA) was connected to the screws. The head-mount was fixed using dental acrylic cement (Lang Dental Manufacturing Co. Inc., Wheeling, IL, USA). At least 7–10 days were allowed for recovery from the surgical procedure. Seizure activity was monitored using the Pinnacle 8401 data conditioning & acquisition system (Pinnacle Technology). Rats were allowed to move freely in the monitoring system during the recordings. Spontaneous recurrent seizures (SRS) were recorded on different days after DFP-induced SE. EEG recordings were reviewed using the Sirenia Seizure Pro software (Pinnacle Technology) by researchers with expertise using this software. An SRS was defined as spike wave discharges (SWD) with amplitude at least twice that of the background EEG activity in awake animals with 5 Hz frequency and a duration of at least 5 s.

2.3. Home cage reactivity

The reactive behavior of subjects towards five different types of tactile stimuli was tested at 1 week, 1 month and 2 month post-exposure using a previously described test (Raffaele et al., 1987). Briefly, subjects were transferred from the vivarium to a procedure room in their home cage and the cage placed into an arena (48 cm × 48 cm × 48 cm) in the center of a sound insulated room dedicated for behavior testing. The cage lid was taken off and the animals were observed for 30 s before applying five types of tactile stimuli in order from least invasive to most invasive: (1) placing corn cob bedding material on the tail; (2) applying light pressure with a plastic rod (30 cm long and 1.25 cm in diameter) to the base of the tail; (3) applying light pressure to the neck; (4) applying light pressure to the tip of the nose; and (5) handling the rat with a gloved hand. Two experimenters blinded to experimental group independently scored the reaction to these stimuli using the following scale: 0, no response to stimuli; 1, forward or backward movement with little reaction; 2, forward or backward movement accompanied by enhanced alertness (erect “Straub” tail or gaze fixed on the investigator); or 3, forward or backward movement with speed and aggression (flinch, flee, forelimb/hind limb bounce, vertical leap, biting at the cage/stick/gloves). Individual scores for each stimuli were added to obtain a total reactivity score for each subject (minimum score = 0, maximum score = 15). The arena was cleaned with 70% ethanol before the beginning of the first test session and after each subject rat was tested, with sufficient time for the ethanol odor to dissipate before the start of the next test session.

2.4. Elevated plus maze

The elevated-plus maze (EPM) is a well-established task for assessing anxiety-like conflict behavior in rodents by allowing subjects to

choose between entering the open arms of the maze (natural exploratory drive) or staying in the safety of the closed arms. The EPM consisted of two closed arms and two open arms, each 45 cm long x 10 cm wide, radiating from a central area (10 cm × 10 cm). The entire apparatus was 45 cm from the floor. A 0.5 cm high lip surrounded the edges of the open arms, whereas the closed arms were surrounded by 20 cm high walls. The EPM was cleaned with 70% ethanol before the beginning of the first test session and after each subject rat was tested, with sufficient time for the ethanol odor to dissipate before the start of the next test session. Room illumination was approximately 30 lx. Subjects were acclimatized to the test room for 1 h prior to testing. At the beginning of each 5 min test session, the subject was placed in the center of the maze facing the open arm and allowed to freely explore for 5 min during which time the activity was recorded using Ethovision video tracking system (EthoVision 10.1, Noldus Information Technology, Leesburg, VA, USA). The total amount of time spent in the open arms as well as the number of entries made into the open arms and closed arms was determined using EthoVision software.

2.5. Open field test

General exploratory locomotion was assessed using the open field test conducted using an arena (48 cm × 48 cm × 48 cm) in the center of a sound insulated room dedicated for behavior testing. The light intensity in the arena was approximately 30 lx. The open field arena was monitored using a video tracking system (EthoVision 10.1, Noldus Information Technology, Leesburg, VA, USA) positioned above the arena. Ethovision software was used to assess locomotor behavior by monitoring the location of the animal relative to a 3 × 3 grid of equal-sized boxes superimposed on the video image of the arena floor. Subjects were acclimatized to the testing room for 1 h prior to being released in the center of the arena, and their behavior was recorded for 15 min. The total distance the subject traveled, the time spent moving and the time spent in the center zone were quantified. A subject was considered to be moving if it traveled with a velocity of ≥1 cm/s.

2.6. Pavlovian fear conditioning

Pavlovian fear conditioning was used to assess learning and memory as previously described (Cowan and Richardson, 2018; Rajbhandari et al., 2018). Animals were trained to associate a conditioned stimulus (CS) with an unconditioned stimulus (UCS) in a chamber (Med-Associates Inc., St. Albans, VT, USA) that was calibrated to deliver foot shocks at 0.7 mA. Each chamber (32 cm wide × 25 cm high × 25 cm deep) had aluminum side walls, a clear polycarbonate front wall, an opaque Plexiglas back wall and ceiling, and a floor composed of stainless steel rods placed 1.6 cm apart. A scrambled shock to the foot was delivered through the floor. Each conditioning chamber was surrounded by a sound attenuating environmental chamber and equipped with an overhead closed circuit television (CCTV) camera to record the subject during each session. Chambers were thoroughly cleaned with 70% ethanol between subjects, and the ethanol odor allowed to dissipate before the start of the next session.

To condition animals, each subject was placed in the chamber with illumination set at 220 lx for 2 min, then presented with an auditory CS (80 dB white noise) for 30 s followed by the UCS, a 3-s foot shock of 0.7 mA delivered through the floor grid. An olfactory cue was added before fear conditioning by dabbing a drop of lemon dish soap solution on the metal tray beneath the grid floor. Each animal was given a total of three CS-UCS pairings with 2 min between each pairing during an 8-min training session. After the training session, animals were placed back in their home cage and returned to the vivarium for 24 h. During conditioning, approximately 50% of the DFP animals did not freeze in response to the stimuli and these animals were excluded from the subsequent cue and context tests. The next day, the memory of the fear-associated context was assessed by placing the animal in the same chamber with identical lighting, visual, floor-texture, and olfactory cues as the day before during tone-shock pairing. The animal's behavior was monitored for 5 min in the absence of an auditory CS and UCS foot shock. The subject rat was then returned to its home cage. On the third day, cued fear conditioning was assessed by placing subject rats into a new context. The scent in the operant chamber was changed to vanilla and the metal floor grid was covered with a transparent Plexiglas sheet on top of a blue paper towel, and the chamber lights dimmed to 7 lx. At the beginning of the 5-min trial, the subject rat was introduced to the chamber and allowed to acclimatize for 2 min before the auditory CS was presented for 3 min without the UCS foot shock. Time spent freezing (defined as the absence of any movement except respiratory movement) during both the context and cue test was manually scored from video recordings at 10 s intervals by two independent investigators blinded to experimental group. Careful analysis of video recordings during scoring revealed no evidence of seizure behavior in DFP animals during the CS-US pairing or the context testing.

2.7. Immunohistochemistry

At the conclusion of all behavioral tests, animals were deeply anesthetized with 4% isoflurane in medical grade oxygen, and subsequently transcardially perfused with 100 ml cold PBS (3.6 mM Na_2HPO_4, 1.4 mM NaH_2PO_4, 150 mM NaCl, pH 7.2)) followed by 100 ml cold 4% paraformaldehyde (PFA) solution in phosphate buffer (0.1 M Na_2HPO_4, 0.1 M NaH_2PO_4, pH 7.2) at a flow rate of 15 ml/min using a Masterflex peristaltic pump (Cole Parmer, Vernon Hills, IL, USA). Brains were removed, blocked in 2-mm thick coronal sections and post-fixed in 4% PFA for 24 h at 4 °C before being transferred to 30% sucrose in PBS and stored at 4 °C for at least 48 h until embedded and flash frozen in Tissue-Plus™ O.C.T. compound (Thermo Fisher Scientific, Waltham, MA, USA). Tissue blocks were cryosectioned into 10-μm thick coronal sections and stored at −80 °C until staining.

All brain sections processed for a specific biomarker were immunostained at the exact same time using the same batch of reagents to ensure comparable experimental conditions across all samples. Slides were brought to room temperature, washed with PBS, placed in 10 mM sodium citrate buffer at pH 6.0 and heated for 30 min in a rice cooker for antigen retrieval. Following antigen retrieval, sections were incubated in blocking buffer, which was 10% normal goat serum (Vector Laboratories, Burlingame, CA, USA), 1% bovine serum albumin (Sigma-Aldrich) and 0.3% Triton X-100 (Thermo Fisher Scientific) in PBS, for 1 h at room temperature, and then incubated with primary antibody in blocking buffer at 4 °C overnight. Primary antibodies included rabbit anti-IBA1 (1:1000, 019–19,741, Wako Laboratory Chemicals, Richmond, VA, USA), mouse anti-CD68 (1:200, MCA341R, Serotec, Hercules, CA, USA), mouse anti-GFAP (1:1000, 3670, Cell Signaling Technology, Danvers, MA, USA), mouse anti-NeuN (1:1000, MAB377, Millipore, Burlington, MA, USA), and rabbit anti-nitrotyrosine (3-NT, 1:200, 06–284, Millipore). Sections were washed in PBS with 0.3% Triton X-100, and then incubated in secondary antibody in blocking buffer for 2 h at room temperature. The secondary antibody used to detect anti-IBA1 was goat-anti rabbit IgG conjugated to Alexa Fluor 568 nm (1:500, 997,761, Life Technologies, Carlsbad, CA, USA); to detect anti-CD68, goat-anti mouse IgG conjugated to Alexa Fluor 488 nm (1:500, A11001, Life Technologies); to detect anti-GFAP or anti-NeuN, goat-anti mouse IgG1(γ1) conjugated to Alexa Fluor 568 nm (1:1000, A21124, Life Technologies); and to detect anti-3-NT, goat-anti rabbit Ig conjugated to Alexa Fluor 488 nm (1:500, Life Technologies A11034). As a negative control, sections were incubated with blocking buffer rather than primary antibody, but otherwise processed identically. All sections were mounted in ProLong™ Gold Antifade Mountant with DAPI (Invitrogen).

Fluorescent images were acquired using the ImageXpress Micro XLS Widefield High-Content Analysis System (Molecular Devices, Sunnyvale, CA, USA). Positive immunostaining was identified as

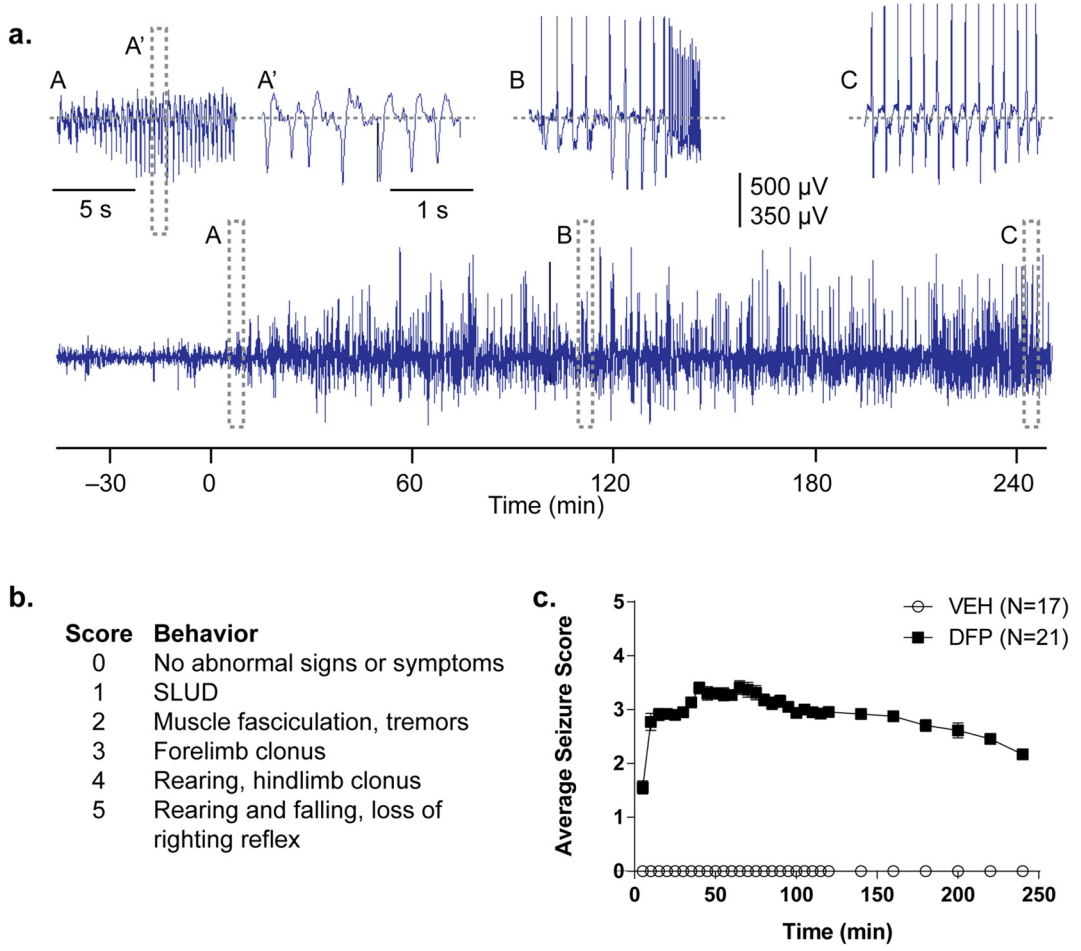

Fig. 2. Acute DFP intoxication elicited robust seizure activity. (a) Representative EEG recording immediately before and following administration of DFP at time zero. The lower trace shows the continuous EEG record (voltage scale, 350 µV). Dashed boxed areas are shown on an expanded scale above (voltage scale, 500 µV). A' shows the dashed boxed area in A on an expanded time scale. Spike-wave activity is evident in A', B and C. (b) Scale used to score the severity of behavioral seizures. SLUD indicates any of the following symptoms of cholinergic activation: salivation, lacrimation, urination, defecation. (c) Seizure scores according to the scheme in B were obtained at 5 min intervals during the first 120 min following administration of vehicle or DFP, and at 20 min intervals between 120 and 240 min post-exposure. Data points correspond to the mean seizure score (± S.E.M.) at each observation time.

fluorescence intensity that was twice the background fluorescence levels in negative control samples. Images were acquired from the basolateral amygdala (Bregma −3.6 to −4.2), dorsolateral thalamus (Bregma −3.0- to −3.6), piriform cortex (Bregma −3.6 to −4.2), hippocampus (Bregma −3.6 to −4.2) and somatosensory cortex (Bregma −3.6 to −4.2) at the same coronal plane across all animals as determined using the photographic atlas of the rat brain (Kruger et al., 1995). Two serial slices were analyzed for each brain region of each animal. Multiple overlapping tiles were stitched together to produce a single image that encompassed an entire brain region that was then processed using automated analysis platforms. All acquired images were used for analysis unless specific brain regions were lost during staining conditions (which occurred in 6 out of 150 images). GFAP immunoreactivity was assessed using ImageJ v1.48 (NIH, USA) to determine the average fluorescence area following a rolling ball background subtraction and binarization of the image. These data are presented as percent area of GFAP relative to time- and brain region-matched samples from VEH animals. IBA-1/CD68 and NeuN/3-NT immunoreactivity were assessed with respect to the percentage of immunopositive cells (identified by DAPI staining) with colocalized immunoreactivity using the Multi Wavelength Cell Sorting Journal within the Custom Module Editor analysis software (MetaXpress High-Content Image Acquisition and Analysis software, version 5.3, Molecular Devices) combined with a self-developed Matlab Script (Matlab 2014b, The Mathworks Inc., Natick, Massachusetts).

2.8. Statistics

Behavior data were analyzed using student's *t*-test, Mann Whitney *t*-test or two-way ANOVA as performed by Prism 6.0 (GraphPad Software, La Jolla, CA, USA). For histological analysis, mixed effects regression models, including animal-specific random effects, were used to assess the differences in primary immunohistochemical outcomes between DFP and VEH animals across brain regions. Exploratory analysis indicated that a natural logarithmic transformation was needed for all outcomes to stabilize the variance and meet the underlying assumptions of the mixed effects models. Outcomes that had a value of zero were shifted by a small positive number prior to taking the natural logarithm. Time post-exposure (1 month or 2 month), exposure group (DFP or VEH), and brain region were all variables of interest in the models. Interactions between these variables were also considered. Akaike information criterion was used for model selection and Wald tests were used to compare each brain region between DFP and VEH groups. Results are presented as geometric mean ratios between DFP and VEH. These ratios may be interpreted as fold changes, so that a ratio of 1.5 corresponds to a 50% increase and a ratio of 0.5 corresponds to a 50% decrease. Point estimates of the ratios and the 95% confidence intervals are presented. When the confidence interval

includes 1, there is no statistical evidence of a difference between the DFP and VEH group. However, when the confidence interval does not include 1, the estimated effect is significant at the 5% level. All analyses were conducted using SAS software version 9.3 (SAS Institute, Inc., Cary, NC, USA) and graphics were created in R version 3.1.0 (R Foundation for Statistical Computing, Vienna, Austria).

3. Results

3.1. Acute DFP intoxication triggers SE that develops into SRS and hyperreactivity in adult male rats

To confirm that the DFP exposure paradigm used in these studies (Fig. 1) triggered robust SE in adult male Sprague-Dawley rats, a subset of animals were implanted with electrodes to measure electroencephalographic activity in the brain during the 4 h immediately following a single s.c. injection of DFP at 4 mg/kg. Changes in normal EEG waveform consistent with SE occurred within minutes of DFP administration and persisted through the entire recording period in all animals implanted with electrodes (Fig. 2a). All DFP-intoxicated animals (both those implanted with electrodes, and those not surgerized for EEG recording) were monitored for seizure behavior as previously described (Siso et al., 2017). All DFP-exposed animals (n = 41/41) exhibited characteristic signs of cholinergic crisis (i.e. SLUD: salivation, lacrimation, urination, defecation) within minutes after intoxication, and consistent with the EEG records, most DFP animals exhibited seizure behavior during the 4 h following DFP exposure (Fig. 2b,c). A maximal seizure score ≥ 3 was observed in 90% of all DFP-exposed animals (n = 37/41). The remaining 10% of DFP-exposed animals that did not exhibit behavioral signs of seizure activity were excluded in further studies. Of the DFP animals that exhibited behavioral seizures, 68% survived 24 h post-exposure, and of those, all survived until euthanized.

There is literature suggesting the development of chronic epilepsy in humans following acute OP intoxication (Waheed et al., 2014). This association has been corroborated in preclinical studies: acute intoxication with the OPs soman or paraoxon triggers the onset of spontaneous recurrent seizures (SRS) in some exposed animals within 5–10 days following OP exposure (de Araujo et al., 2010, 2012; Shrot et al., 2014). Consistent with these observations, we observed seizure behavior in DFP animals at delayed times post-exposure. To determine whether behavioral signs of seizures were indicative of electroencephalographic seizures, a subset of DFP animals exhibiting seizure behavior were implanted with electrodes at ~ 2 months post-exposure. Monitoring of electrographic activity at 100 days post-intoxication indicated abnormal EEG activity consistent with seizure activity (Fig. 3a). Of the six animals instrumented for this experiment, all six exhibited SRS by 100 days post-intoxication (Fig. 3b), although the rates at which animals experienced SRS varied between animals (Fig. 3c).

DFP animals also exhibit hyperreactive responses to physical and auditory stimuli. To quantify these observations, we adapted a previously described reactivity test (Raffaele et al., 1987) that uses a ranking system of the animal's reaction to five types of stimuli from 0 (no reaction) to 3 (aggressive response) to derive a summed score across all five stimuli. Using this test, we compared the reactivity of DFP versus VEH animals at 1 week, 1 month and 2 months post-exposure. DFP animals were significantly more reactive than VEH animals beginning as early as 1 week (mean ± SD: VEH 2.55 ± 2; DFP 9.37 ± 2.22), and this difference persisted at 1 (mean ± SD: VEH 2.75 ± 2.7; DFP 7.16 ± 2.63), and 2 months (mean ± SD: VEH 1.65 ± 2; DFP 4.79 ± 3.27) post-exposure (Fig. 3d).

3.2. Acute DFP intoxication induces persistent behavioral changes

Anxiety-like behavior, general locomotor and exploratory behavior, and learning and memory were assessed in DFP and VEH animals at 1 and 2 months post-exposure. Different cohorts were assessed at the two time points, with all three behaviors assessed in each cohort. To minimize carryover effects, behavioral tasks were performed in the order of least stressful to most stressful in all cohorts (Fig. 1b), and experiments were conducted in two cohorts per time point to confirm reproducibility.

Anxiety-like behavior was assessed using the elevated plus maze (EPM). DFP animals spent a greater percentage of time on the open arms compared to VEH at both 1 month (Fig. 4a; VEH: 5.9 ± 2.14%; DFP: 26.5 ± 6.5%) and 2 months post-exposure (Fig. 4d, VEH: 22.6 ± 5.31%; DFP: 58.7 ± 11.8%). No significant treatment effects on the number of open arm entries or total arm entries at either 1 month (Fig. 4b, VEH: 2.4 ± 1.83; DFP: 5.14 ± 3.84; Fig. 4c, VEH: 14.3 ± 1.11; DFP: 14.7 ± 2.73) or 2 months (Fig. 4e, VEH: 3.8 ± 0.63; DFP: 7.75 ± 1.99; Fig. 4f, VEH: 12.1 ± 0.77; DFP: 12.75 ± 2.29) post-exposure were observed. Greater percentage of time on the open arms indicates low anxiety-like behavior in DFP compared to VEH at 1 and 2 months post-exposure. No effect on the number of total entries supports that this finding is attributable to changes in anxiety-like behavior and not a confound of low activity.

General exploratory and locomotor behavior was assessed using the open field test. The total distance traveled, the total amount of time the animal spent moving and the percent of time the animal spent in the center of the open field were measured. No significant differences were observed between VEH and DFP animals on any of these endpoints at 1 (Fig. 5a, VEH: 2.75 ± 0.42 m; DFP: 3.15 ± 1.18 m; Fig. 5b, VEH: 10.6 ± 1.13 min; DFP: 9.42 ± 2.58 min; Fig. 5c, VEH: 1.44 ± 0.85 min; DFP: 1.72 ± 1.5 min) or 2 months post exposure (Fig. 5d, VEH: 2.7 ± 0.49 m; DFP: 3.5 ± 2.15 m; Fig. 5e, VEH: 8.95 ± 0.85 min; DFP: 8.85 ± 4.13 min; Fig. 5f, VEH: 1.3 ± 0.81 min; DFP: 1.92 ± 1.16 min).

Pavlovian fear conditioning was used to assess the effect of acute DFP intoxication on learning and memory. This task is a form of associative learning that pairs an unconditioned stimulus (foot shock) with a conditioned stimulus (auditory cue). Learning and memory is measured as the percentage of time the subject freezes when subsequently exposed to the same context or cue: increased percent time freezing indicates stronger learning and memory. On the first day of the behavioral test, animals were trained to associate the unconditioned stimulus with the conditioned stimulus. Of the animals included in the analysis (see Methods section), there was a significant effect of the training task in both the VEH and DFP animals at each time point (1 and 2 months post-exposure) as determined by two-way ANOVA (1 month & 2 month: $p < .001$) (Fig. 6a, b). There were no exposure-related effects on the freezing response during conditioning on the first day (two-way ANOVA, 1 month: $p = .26$, 2 month: $p = .2$) and there was no significant interaction between DFP exposure and training phase (two-way ANOVA, 1 month: $p = .18$, 2 month: $p = .06$).

During the context test, there was no significant difference in the percentage time spent freezing between the DFP and VEH animals at 1 month post-exposure (DFP: 38 ± 8.9%; VEH: 50 ± 6.7%, t-test, $p = .34$) (Fig. 6a); however, at 2 months post-exposure, DFP animals spent significantly less time freezing than VEH animals (DFP: 19 ± 5.56%; VEH: 46 ± 6.13%, t-test, $p < .05$) (Fig. 6b). During the cue test, the percentage time spent freezing was significantly less for DFP animals relative to VEH animals at both 1 month (DFP: 41 ± 10.9%; VEH: 76 ± 8.01%, t-test, $p < .05$) and 2 months (DFP: 45 ± 13.6%; VEH: 79 ± 7.23%, t-test, $p < .05$) post-exposure (Fig. 6).

3.3. DFP causes persistent neuroinflammation and oxidative stress in multiple brain regions

Acute DFP intoxication causes substantial neurodegeneration in multiple brain regions that begins as early as 4 h post-intoxication (Li et al., 2011), peaks at approximately 1 week post-exposure and largely subsides between 2 and 3 weeks after exposure (Siso et al., 2017). These

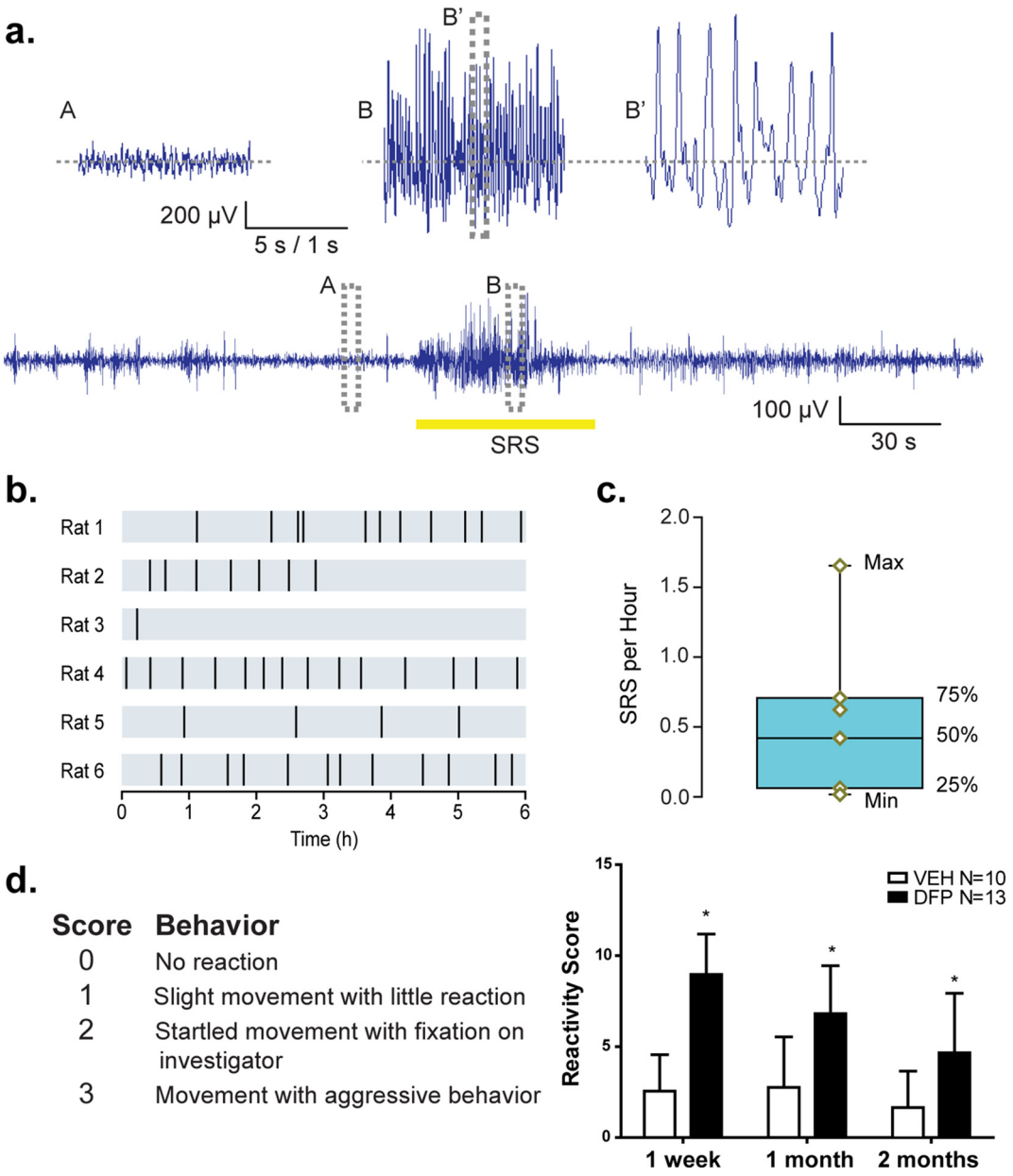

Fig. 3. Acute DFP intoxication caused animals to develop spontaneous recurrent seizures (SRS) and exhibit hyperreactive behavior. (a) Representative electroencephalogram (EEG) of SRS in a DFP rat at 100 days post-DFP exposure. The lower trace shows the continuous EEG record (voltage scale, 100 µV). Dashed boxed areas are shown on an expanded scale above (voltage scale, 200 µV). B′ shows the dashed boxed area in B on an expanded time scale. The yellow bar in the bottom trace depicts an episode of a SRS. (b) Raster plot depicting the number of occurrences of SRS recorded over a 6 h period in DFP rats at 100 days post-DFP exposure. (c) A box plot illustrating the frequency of SRS that occurred per hour in DFP animals (n = same 6 animals shown in panel b). (d) Behavioral assessment of reactivity revealed observable aggression in DFP animals beginning as early as 1 week post-exposure that persisted up to 2 months post-exposure. Animals were scored for reactions to five different tactile stimuli and the score for each stimulus was summed to determine the total score with 0 indicating negligible reactivity and 15 representing maximal reactivity. Data presented as mean ± SD. *Significantly different from time-matched vehicle control at $p < .05$ as determined by Mann Whitney U test.

neurodegenerative consequences are accompanied by a robust neuroinflammatory response in the hippocampus and cortex (Li et al., 2015; Rojas et al., 2015; Siso et al., 2017) characterized by microglial and astrocyte activation that persists at 1 and 2 months post-exposure (Flannery et al., 2016; Siso et al., 2017). To confirm these earlier observations with more robust, non-biased quantification, we used automated image acquisition and analysis to quantify reactive astrogliosis and microgliosis in multiple brain regions of DFP animals at 1 and 2 months post-exposure. Also, while neuroinflammation and oxidative stress often co-exist, oxidative stress has only been examined in the rat model of acute DFP intoxication out to 72 h post-exposure (Kim et al., 1999; Liang et al., 2018; Zaja-Milatovic et al., 2009). Therefore, we also examined 3-NT immunoreactivity, a biomarker of oxidative stress (Ahsan, 2013) at 1 and 2 months post-exposure in the same brains examined for reactive astrogliosis and microgliosis.

Increased GFAP immunoreactivity, a biomarker of reactive astrocytes, was observed in multiple brain regions (Fig. 7), and these effects were bilaterally symmetrical. Automated image acquisition and analysis was used to quantify the percent area of GFAP immunoreactivity in the basolateral amygdala, somatosensory cortex, piriform cortex, dorsal lateral thalamus, and hippocampus of DFP and VEH animals at 1 and 2 months post-exposure. No statistically significant differences were

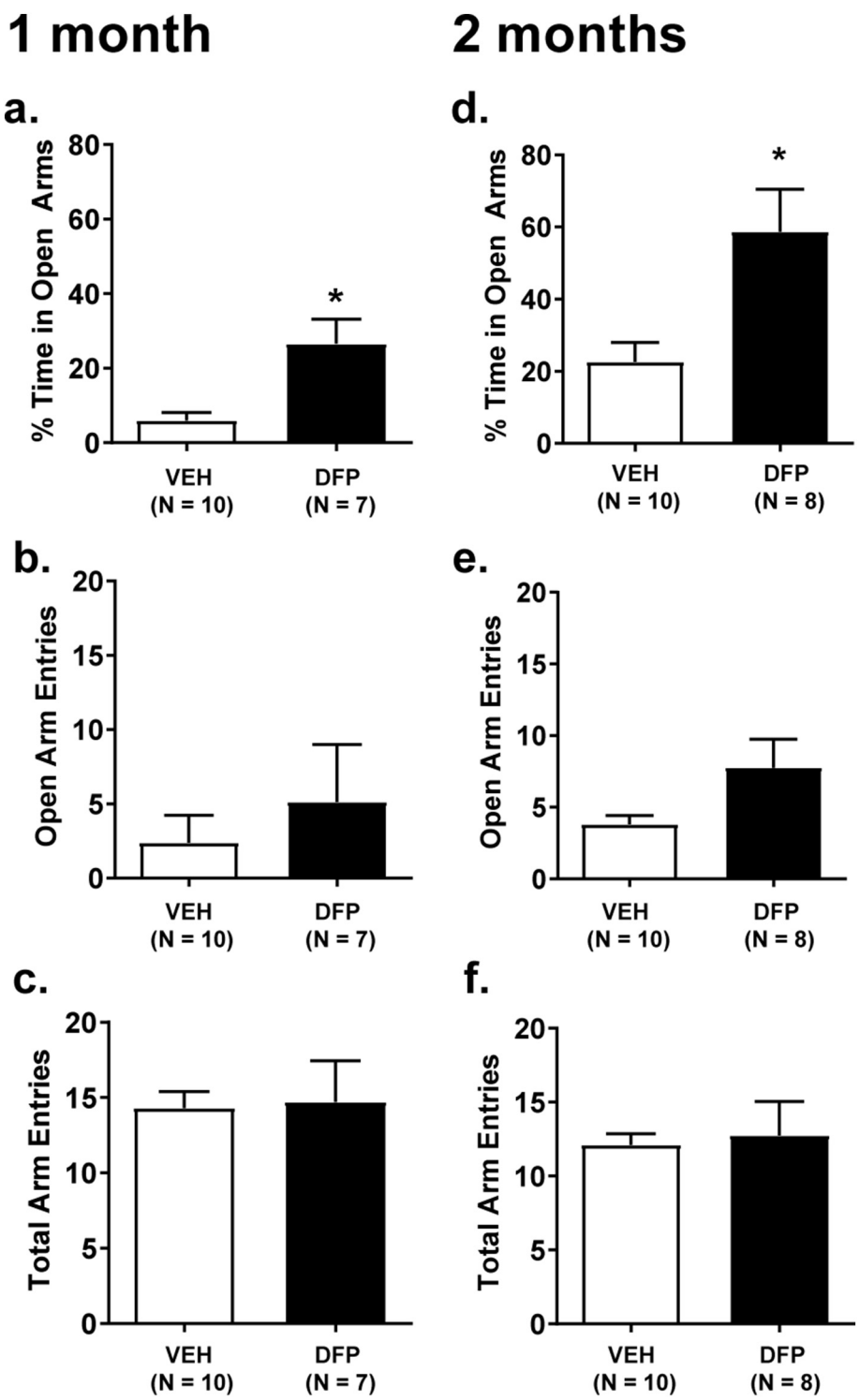

Fig. 4. Acute DFP intoxication caused persistent anxiolytic effects. The performance of DFP animals in the elevated plus maze was altered relative to vehicle controls such that the DFP animals spent significantly more time in open arms of the maze (a, d). However, acute DFP intoxication did not change the number of open arm (b, e) or total arm entries (c, f) at either 1 or 2 months post-exposure. Data presented as mean ± S.E.M. *Significantly different from vehicle control at $p < .05$ as determined by student's *t*-test.

found between VEH animals at 1 month versus 2 month post-exposure as determined by 1 way ANOVA; therefore, animals from these two cohorts were combined into a single VEH control group for further histological analyses. The geometric mean ratio was calculated for the GFAP area in each brain region of DFP animals relative to VEH animals (Fig. 7b). Difference in the area of GFAP immunoreactivity between DFP and vehicle animals did not differ by time post-exposure or brain region. There was a 1.7-fold increase in the GFAP staining area in DFP treated animals relative to vehicle animals that persisted at 1 and 2 months following exposure across all the five brain regions that were analyzed.

Early astrogliosis has been shown to accompany a period of robust microglial activation in the hippocampus and cortex of DFP-exposed rats (Flannery et al., 2016); therefore, we also quantified microgliosis.

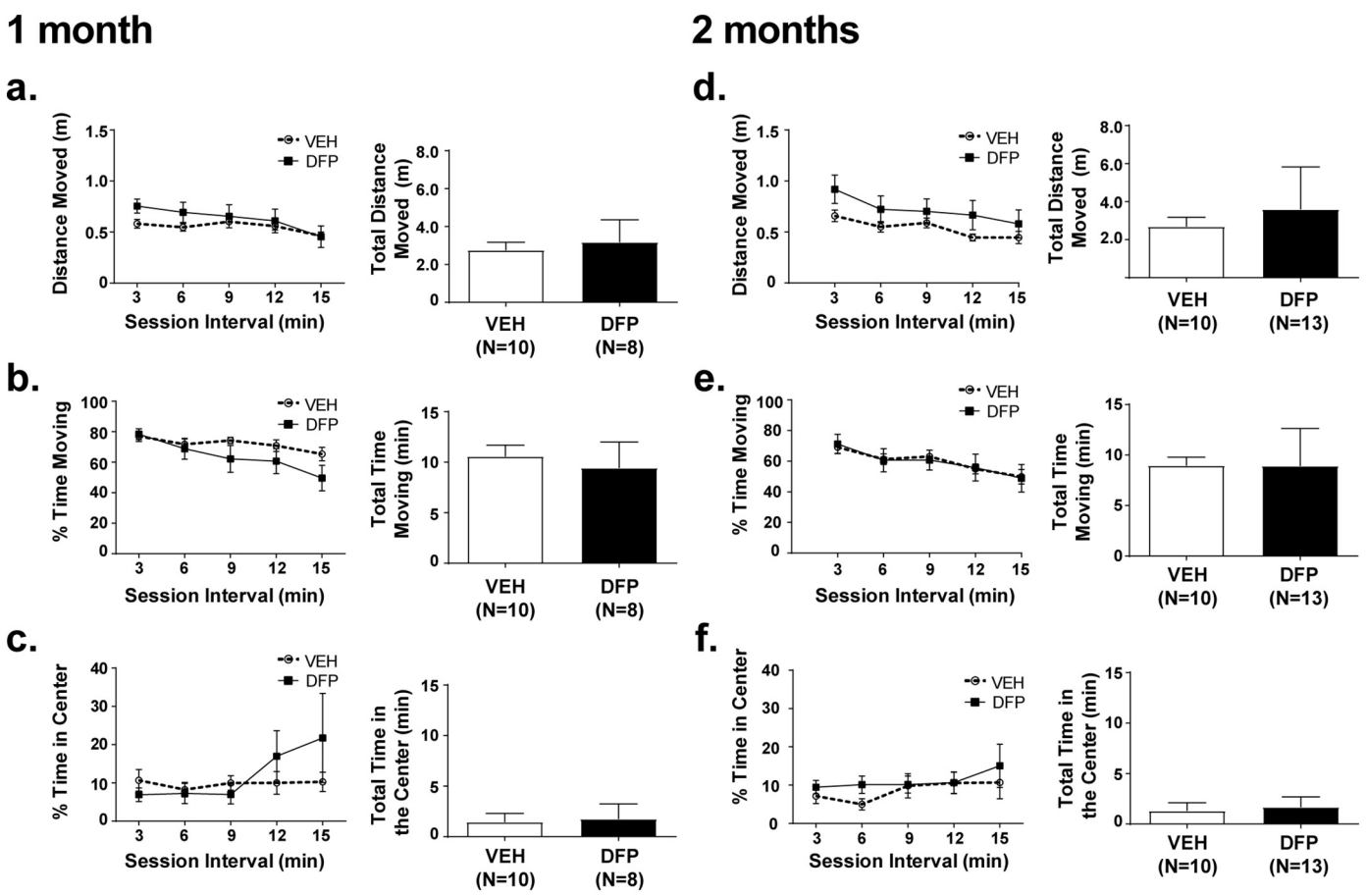

Fig. 5. General locomotor activity and exploratory behavior were not significantly altered by acute DFP intoxication. Parameters measured in the open field test included: (a, d) total distance traveled; (b, e) the percentage of the session time the animal spent moving; and (c, f) the percentage of time the animal spent in the center of the testing chamber. Data presented as mean ± SD. "NS" denotes no significance from vehicle control at $p = .05$ as determined by unpaired student's *t*-test.

IBA-1 immunoreactivity, a pan microglia biomarker, and CD68 immunoreactivity, a biomarker of phagocytically active microglia, were quantified within the basolateral amygdala, somatosensory cortex, piriform cortex, dorsal lateral thalamus and hippocampus of DFP and VEH animals at 1 month and 2 months post-exposure. Bilaterally symmetrical increases in microgliosis were observed in multiple brain regions (Fig. 8). The total percentage of cells that were IBA-1 immunopositive and the percentage of IBA-1 immunopositive cells that were co-labeled for CD68 immunoreactivity were quantified in each brain region using automated image acquisition and analysis. The geometric mean ratio of these values from DFP animals compared to VEH control was calculated for each brain region (Fig. 8b, c). Difference between DFP and VEH animals with respect to the percentage of IBA-1 immunopositive cells that were immunoreactive for CD68 differed by time post-exposure and brain region. There was a significant difference in DFP versus VEH animals at 1 month, but not at 2 months post-exposure in the basolateral amygdala, somatosensory cortex and hippocampus, and there were no significant differences between DFP and VEH animals in the piriform cortex or thalamus at either 1 or 2 months post-exposure (Fig. 8b). The percentage of cells immunoreactive for IBA-1 was significantly different between DFP and VEH animals in all brain regions at 1 month post-exposure; however, at 2 months post-exposure, this difference only remained significant in the piriform cortex (Fig. 8c).

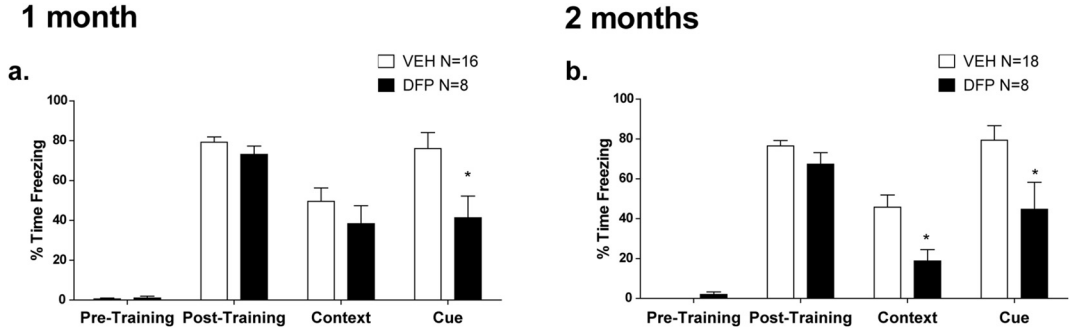

Fig. 6. Pavlovian fear conditioning revealed persistent learning and memory deficits in DFP-intoxicated animals. DFP animals showed decreased freezing behavior in cued conditioning at 1 month post-exposure (a) that persisted at 2 months post exposure (b). Deficits in contextual fear conditioning were observed at 2 months post-exposure (b). Data presented as mean ± S.E.M. *Significantly different from vehicle control at $p < .05$ as determined by two way ANOVA. No statistically significant treatment-related differences were identified in the training phase using two-way ANOVA ($p > .05$).

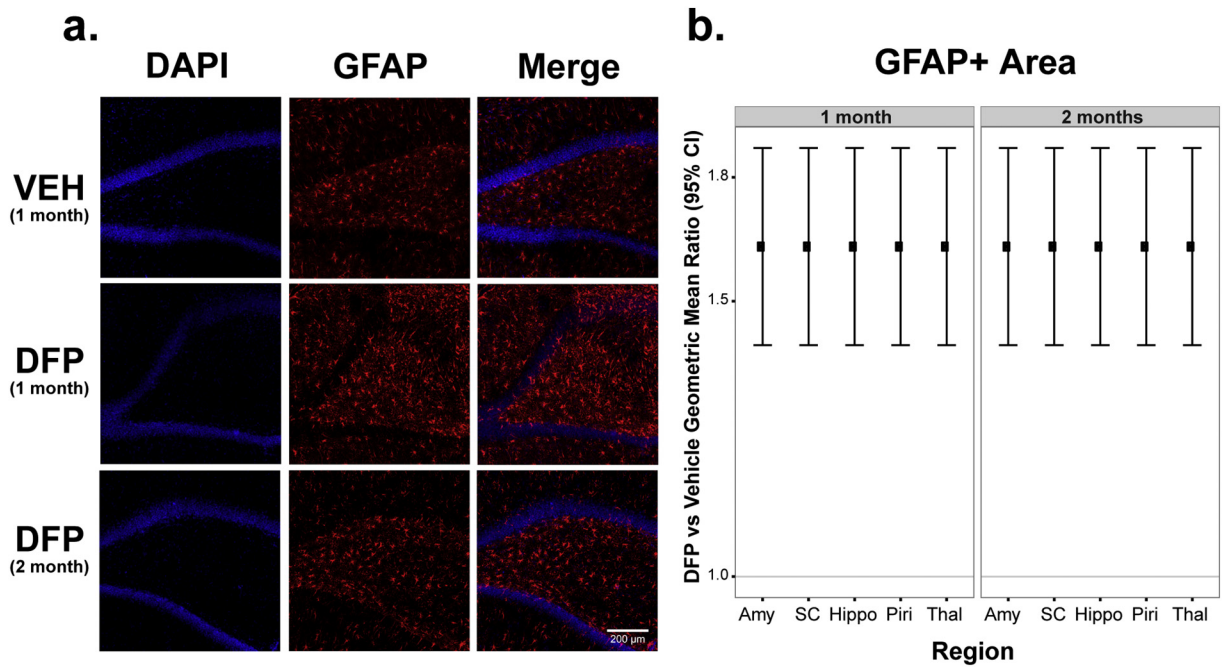

Fig. 7. Acute DFP intoxication triggered persistent reactive astrogliosis in multiple brain regions.
(a) Representative micrographs of GFAP immunoreactivity in the hippocampus of adult male rats exposed to vehicle (VEH) or DFP. Brain sections were labeled with DAPI (blue) to identify cell nuclei and immunostained for GFAP (red) to identify astrocytes. Bar = 200 µm. (b) Geometric mean ratio (dot) of the area of GFAP immunoreactivity in DFP relative to VEH animals with 95% confidence intervals (bars) (n = 14 DFP and 13 VEH). The y-axis is a log scale. Confidence intervals that do not include 1 (identified as the grey line) indicate a significant difference between DFP and VEH groups. Amy = amygdala; SC = somatosensory cortex; Hippo = hippocampus; Piri = piriform cortex; Thal = dorsal lateral thalamus. (For interpretation of the references to colour in this figure legend, the reader is referred to the web version of this article.)

It is well established that activated microglia and astrocytes increase production of reactive oxygen and nitrogen species that positively feedback to perpetuate a proinflammatory response (Lugrin et al., 2014). To determine whether the persistent neuroinflammatory response observed in multiple brain regions of the DFP animal correlated with increased oxidative stress at these delayed times post-exposure, we quantified 3-NT immunoreactivity. 3-NT is a well-established marker of oxidative damage, which typically results from the reaction of peroxynitrite with free or protein-bound tyrosine residues within the cell (Ahsan, 2013). Automated image acquisition and analysis of 3-NT and NeuN, a biomarker of neurons, revealed an elevated and prolonged, bilaterally symmetrical oxidative stress response in multiple brain regions of DFP animals compared to VEH controls (Fig. 9). The geometric mean ratio of the ratio of NeuN immunopositive cells that were also immunoreactive for 3-NT was calculated for DFP animals compared to the VEH group (Fig. 9b). There was a significant increase in the percentage of NeuN immunopositive cells that expressed 3-NT in the somatosensory cortex, hippocampus and dorsal lateral thalamus of DFP versus VEH animals at 1 and 2 months post-exposure (Fig. 9b). In contrast, there was no significant effect of DFP on the percentage of 3-NT immunoreactive neurons in either the amygdala or piriform cortex at either time post-exposure. Global levels of oxidative stress were also assessed by quantifying the colocalization of 3-NT immunoreactivity with DAPI. The geometric mean ratio of 3-NT and DAPI colocalization was calculated for DFP animals compared to the VEH group (Fig. 9c). The percentage of 3-NT immunoreactive cells was significantly increased in the somatosensory cortex, piriform cortex, hippocampus, and dorsal lateral thalamus of DFP animals compared to VEH controls at 1 and 2 months post-exposure (Fig. 9c). However, there were no significant effects of DFP on global 3-NT expression in the basolateral amygdala.

4. Discussion

Previous studies of adult male rats demonstrated that DFP-induced SE triggers a robust neuroinflammatory response (Flannery et al., 2016; Kuruba et al., 2018; Li et al., 2015; Li et al., 2011; Liu et al., 2012; Rojas et al., 2015; Siso et al., 2017; Wu et al., 2018) and increases oxidative stress in the brain (Kim et al., 1999; Liang et al., 2018; Zaja-Milatovic et al., 2009) during the first few days post-exposure. We also previously showed that increased GFAP and IBA-1 immunoreactivity persist in multiple brain regions for up to 2 months post-exposure (Flannery et al., 2016; Siso et al., 2017). In addition, deficits in memory (Brewer et al., 2013; Flannery et al., 2016; Rojas et al., 2016) and changes in depression-relevant behavior (Wright et al., 2010) have been reported in the weeks following acute exposure to DFP. Here, we extend these previous observations of the rat DFP model by demonstrating coincident neuroinflammation and oxidative stress in multiple brain regions that persist at 1 and 2 months post-exposure. Furthermore, DFP-intoxicated animals who survive SE go on to develop SRS, hyperreactivity to tactile stimuli, cognitive deficits and anxiolytic behavior that also persist for at least 2 months post-exposure.

Consistent with earlier reports (Deshpande et al., 2010; Li et al., 2011; Pouliot et al., 2016; Rojas et al., 2015), we observed that a single s.c. injection of DFP at 4 mg/kg triggered SE in adult male rats within minutes of exposure, as confirmed by both EEG and behavioral criteria. Humans who survived acute sarin intoxication in the 1995 Tokyo subway attacks exhibited EEG abnormalities years after exposure (Okumura et al., 2005). Preclinical observations demonstrating that rats develop SRS after SE induced by soman (de Araujo et al., 2010) or paraoxon (Shrot et al., 2014) suggest these events may be causally linked. Anecdotal evidence from our previous studies suggested that rats acutely intoxicated with DFP similarly develop SRS (Siso et al., 2017). Here, we confirmed these preliminary observations in a subset of animals instrumented for EEG analyses. While SRS was detected in all (6/6) of the animals examined, the sample size was small and biased in

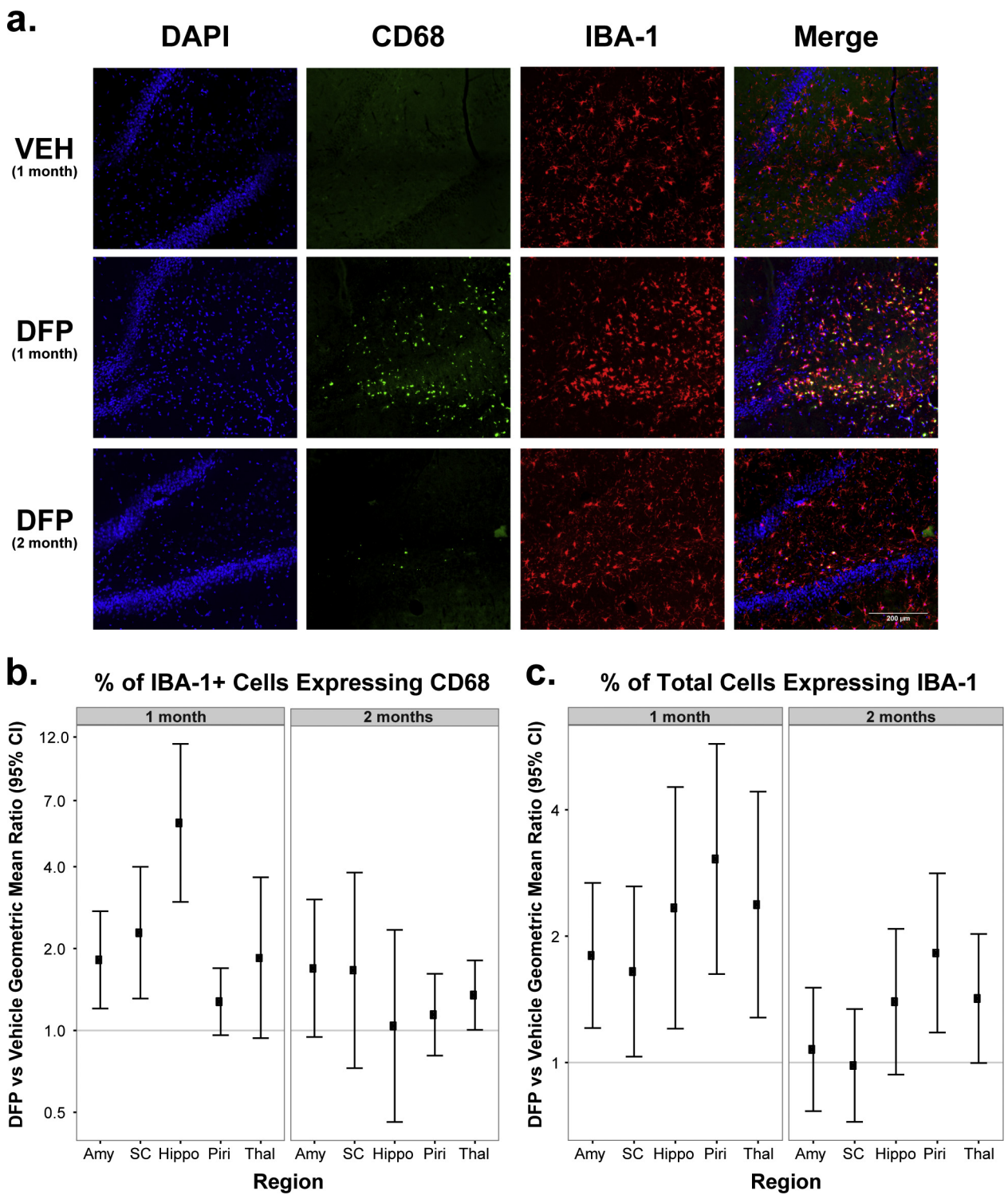

Fig. 8. Acute DFP intoxication triggered microglial activation. (a) Representative micrographs of CD68 and IBA-1 immunoreactivity in the hippocampus of adult male rats exposed to vehicle (VEH) or DFP. Brain sections were labeled with DAPI (blue) to identify cell nuclei and immunostained for both CD68 (green) and IBA-1 (red) to identify activated microglia. Bar = 200 µm. (b) Geometric mean ratio (dot) of the percentage of IBA-1 immunoreactive cells co-reactive for CD68 and IBA-1; and (c) percentage of total cells per unit area that were IBA-1 immunoreactive in DFP relative to VEH animals with 95% confidence intervals (bars) (1 month: $n = 6$ DFP and 5 VEH; 2 months: $n = 8$ DFP and 6 VEH). The y-axis is a log-scale. Confidence intervals that do not include 1 (grey line) indicate a significant difference between DFP and VEH groups. Amy = amygdala; SC = somatosensory cortex; Hippo = hippocampus; Piri = piriform cortex; Thal = dorsal lateral thalamus. (For interpretation of the references to colour in this figure legend, the reader is referred to the web version of this article.)

that animals were selected for this experiment because they were exhibiting seizure-like behavior. Thus, additional studies with a larger sample size are needed to determine the percentage of DFP intoxicated rats that develop SRS and to characterize the developmental timeline of DFP-induced SRS. Data from such studies will inform mechanistic studies to understand how SRS develops following OP-induced SE, and will provide insights into the therapeutic window for preventing the onset of acquired epilepsy in OP-intoxicated individuals.

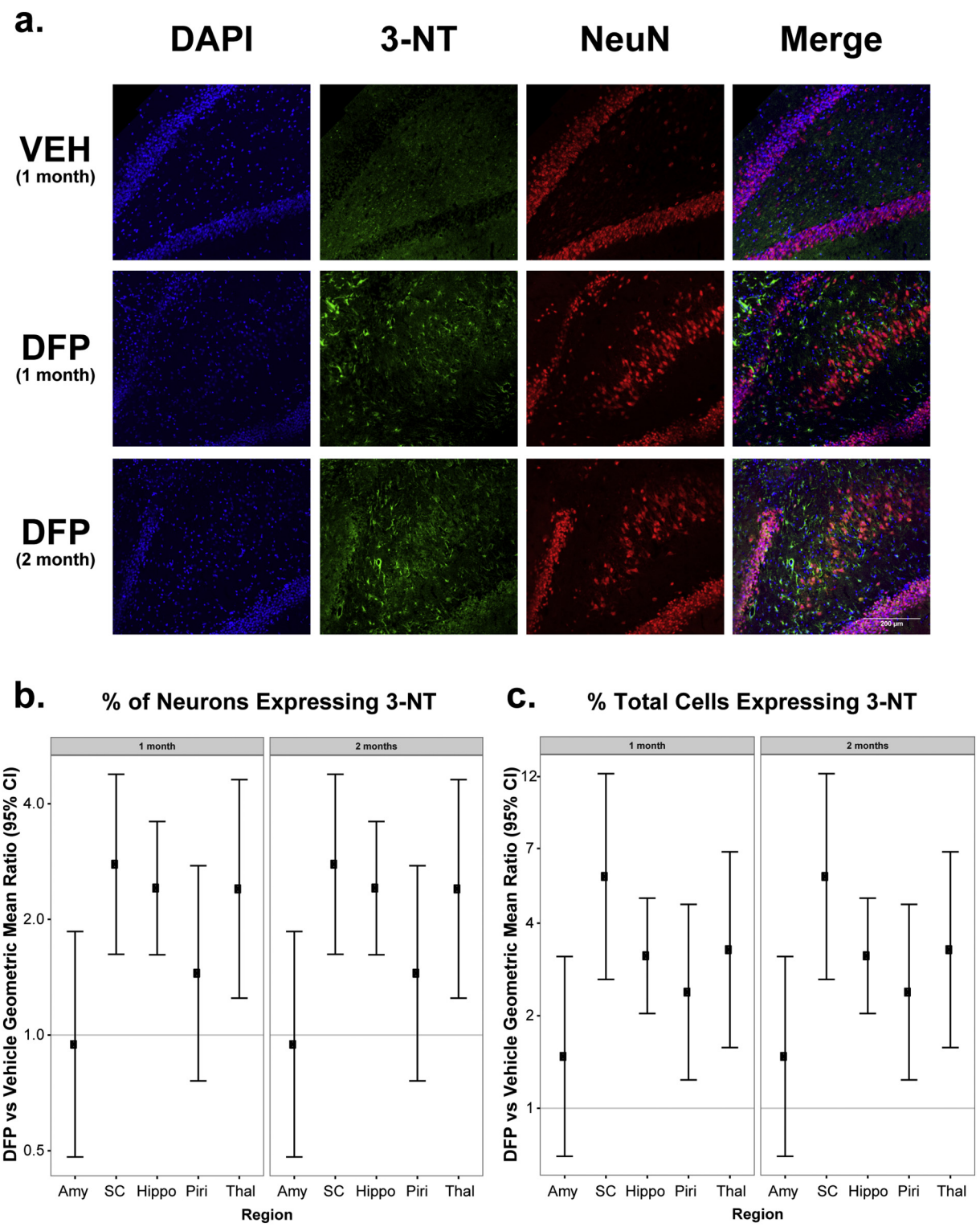

Fig. 9. Acute DFP intoxication causes persistent oxidative stress in multiple brain regions. (a) Representative micrographs of 3-NT and NeuN immunoreactivity in the hippocampus of adult male rats exposed to vehicle (VEH) or DFP. Brain sections were labeled with DAPI (blue) to identify cell nuclei and immunostained for 3-nitrotyrosine (3-NT, green) as a biomarker of oxidative stress and NeuN (red) to identify neurons. Bar = 200 µm. (b, c) Geometric mean ratio of the percentage of neurons (b) and of total cells (c) expressing 3-NT in DFP relative to VEH animals with 95% confidence intervals (bars) (n = 15 DFP and 9 VEH). The y-axis is a log-scale. Confidence intervals that do not include 1 (grey line) indicate a significant difference between DFP and VEH groups. Amy = amygdala; SC = somatosensory cortex; Hippo = hippocampus; Piri = piriform cortex; Thal = dorsal lateral thalamus. (For interpretation of the references to colour in this figure legend, the reader is referred to the web version of this article.)

The findings of this study indicate that with the possible exception of effects on anxiety-like behavior, the rat model of acute DFP intoxication recapitulates many of the neurologic sequelae documented in human survivors of acute OP intoxication and in preclinical models of acute intoxication with OP warfare agents (Chen, 2012; de Araujo et al., 2012; Pereira et al., 2014). Persistent memory impairment is one of the most common behavioral consequences observed in humans who survive acute OP poisoning (Chen, 2012; Okumura et al., 2005). Years after the 1995 sarin attack in the Tokyo subway, exposed rescue personnel and subway workers exhibited significant deficits on memory tests compared to non-exposed control subjects (Miyaki et al., 2005; Nishiwaki et al., 2001). Memory deficits have been previously reported in the rat model of acute DFP intoxication at 1 month post-exposure using Pavlovian fear conditioning (Flannery et al., 2016) or Morris water maze (Brewer et al., 2013) and at 3 months post-exposure using novel object recognition (Rojas et al., 2016). Our findings corroborate these earlier studies by demonstrating that acute DFP intoxication impairs memory in the Pavlovian fear conditioning task at both 1 and 2 months post-exposure. These performance deficits are not secondary to impaired motor activity since DFP animals did not show locomotor deficits in the open field test. Interestingly, at 1 month post-exposure, DFP animals exhibited deficits in the cue but not context test, whereas at 2 months post-exposure, DFP animals showed deficits in both the cue and context test. The context test is predominantly hippocampal-dependent whereas the cue test relies on both hippocampal and amygdalar function. Thus, this observation suggests that acute DFP intoxication causes progressive brain damage that varies between brain regions.

Human survivors of acute OP intoxication are reported to experience significant high levels of anxiety for years after exposure (Hayden et al., 2010; Levin et al., 1976; Yokoyama et al., 1998). Preclinical studies demonstrate that acute intoxication with the OP warfare agent soman similarly results in persistent anxiety-like behavior (Coubard et al., 2008; Prager et al., 2014). Soman-induced anxiety-like behavior is linked to neuronal loss in the basolateral amygdala, decreased ratio of interneurons to the total number of neurons, as well as a reduction in background inhibitory activity (Prager et al., 2014). Acute DFP intoxication similarly causes significant neuronal cell loss in the amygdala (Siso et al., 2017), so why DFP should cause anxiolytic as opposed to anxiogenic effects remains uncertain. However, results from preclinical models of acute intoxication with OP pesticides suggest that effects on anxiety-like behavior vary depending on the OP and/or dose. For example, acute intoxication with paraoxon at doses that triggered SE caused persistent anxiogenic behavior in rodents for up to 3 months following exposure (Deshpande et al., 2014); however, studies of chlorpyrifos suggest that exposed animals may develop anxiogenic or anxiolytic behavior depending on the dose and time post-exposure (Lopez-Crespo et al., 2009). Other groups have shown that exposure to seizurogenic (Rojas et al., 2016) or non-seizurogenic (Wright et al., 2010) doses of DFP that cause cholinergic symptoms induces short-term anxiolytic behavior in rats. Our data extend these findings by demonstrating that the anxiolytic effects of acute DFP intoxication persist at 1 and 2 months post-exposure. These data add to the growing preclinical literature suggesting variable effects of OP intoxication on anxiety depending on the exposure paradigm. Whether this is also true in humans has yet to be determined.

Many have posited that the SRS and neurobehavioral consequences of OP-induced SE are mediated at least in part by neuroinflammation (Collombet, 2011; de Araujo et al., 2012; Guignet and Lein, 2018) and/or oxidative stress in the brain (Pearson and Patel, 2016; Vanova et al., 2018). These hypotheses are driven in large part by preclinical data demonstrating that OP-induced behavioral impairments are often preceded by or coincident with robust neuroinflammation (Collombet, 2011, de Araujo et al., 2012, Guignet and Lein, 2018) and upregulated expression of oxidative stress biomarkers in the brain (Kim et al., 1999; Liang et al., 2018; Zaja-Milatovic et al., 2009). Our previous histological and in vivo PET imaging studies demonstrated that DFP triggers pronounced reactive astrogliosis and microglial activation in multiple brain regions that persist at 1 and 2 months post-exposure (Flannery et al., 2016; Siso et al., 2017). The data reported here, which differed from these previous studies by using automated image analysis to quantify immunoreactivity, incorporating CD68 immunoreactivity to identify phagocytic microglia, and co-labeling for biomarkers of oxidative stress, largely confirm our previous observations. As reported previously (Siso et al., 2017), there is spatiotemporal heterogeneity of the neuroinflammatory response triggered by acute DFP intoxication. Here, we observed DFP-induced SE significantly increased GFAP immunoreactivity at both 1 and 2 months post-exposure in all the brain regions examined, which included the somatosensory cortex, piriform cortex, hippocampus, thalamus, and amygdala. In contrast, IBA-1 immunoreactivity was significantly increased in all five brain regions at 1 month-post-exposure, but by 2 months post-exposure, had returned to VEH control levels in all but the piriform cortex, where it remained elevated. Analyses of the phagocytic status of microglia cells by CD68 immunoreactivity, which is thought to represent fully activated microglia (Guignet and Lein, 2018), revealed significantly increased numbers of phagocytic microglia only in the amygdala, somatosensory cortex and hippocampus, and only at 1 month post-exposure. This perhaps reflects the fact that in the DFP intoxicated animal, neurodegeneration has largely subsided by 14 days post-exposure (Siso et al., 2017).

Neuroinflammation and oxidative stress are inextricably linked processes (Guignet and Lein, 2018) and there is growing interest in the functional relationship between these in the context of acute OP intoxication. The brain is particularly susceptible to oxidative stress, which is defined as the imbalance between the production and detoxification of reactive oxidative species, because of its high composition of lipids, high energy demand and lower levels of cellular antioxidant systems (Pearson and Patel, 2016). Excessive production of reactive oxidative species that overwhelms endogenous antioxidant processes is associated with neuronal cell death as well as reactive astrogliosis and microglial activation (Pearson and Patel, 2016). Activated astrocytes and microglia also contribute to oxidative stress by secreting reactive oxidative species (Guignet and Lein, 2018; Wilkinson and Landreth, 2006). Acute DFP intoxication has been shown to elevate levels of reactive oxygen and nitrogen species in the brain during the first few hours post-exposure, and this response correlates with dendritic atrophy and neurodegeneration in the hippocampus and cortex (Kim et al., 1999, Liang et al., 2018, Zaja-Milatovic et al., 2009). Our data indicate that oxidative stress, as determined by 3-NT immunoreactivity, persisted in many brain regions for as long as 2 months post-DFP exposure. However, the spatiotemporal pattern of oxidative stress triggered by acute DFP intoxication varied from that of neuroinflammation in that 3-NT immunoreactivity was not significantly increased in the amygdala at either 1 or 2 months post-exposure. Both neurons and non-neuronal cells appear exhibited signs of oxidative stress in the somatosensory cortex, hippocampus and thalamus, as indicated by co-localization of 3-NT and NeuN immunoreactivity. In contrast, increased oxidative stress observed in the piriform cortex predominantly affects non-neuronal cells.

There are few data regarding the temporal and mechanistic relationships of either neuroinflammation or neurodegeneration to oxidative stress in the context of acute OP intoxication. A study of the spatiotemporal profile of the expression of oxidative stress biomarkers (specifically, the ratio of reduced to oxidized glutathione and levels of nitrosylated tyrosine) in rats acutely intoxicated with DFP reported increased oxidative stress in the brain at 24 and 48 h post-exposure, but not at 6 and 12 h post-exposure (Liang et al., 2018). Considered in light of studies that have reported neuroinflammation in preclinical models of acute DFP intoxication as early as 1–2 h post-exposure (Li et al., 2015; Liu et al., 2012), these data suggest that neuroinflammation may be driving oxidative stress. However, treatment of rats acutely

intoxicated with DFP with a catalytic antioxidant administered at 5 or 15 min post-exposure significantly attenuated (but did not completely block) both oxidative stress and neuroinflammation, the latter determined by levels of proinflammatory cytokines in the brain, and these effects coincided with decreased neurodegeneration (Liang et al., 2018). While acknowledging the caveat that in the current study we only examined one measure of oxidative stress, our observation that increased GFAP and IBA-1 immunoreactivity persisted in the amygdala in the absence of increased 3-NT immunoreactivity suggests that oxidative stress is not necessary for maintaining neuroinflammation, and that neuroinflammation does not necessarily trigger oxidative stress. The latter is consistent with the hypothesis that neuroinflammation is neurotoxic early after OP-induced SE but shifts to being neuroprotective at late time points post-exposure (Banks and Lein, 2012; Collombet, 2011; Guignet and Lein, 2018). Collectively, these observations suggest that the functional relationships between neuroinflammation, oxidative stress and neurodegeneration are dynamic over time post-exposure (Guignet and Lein, 2018). Determining how these relationships change will be important for identifying therapeutic windows.

In conclusion, we have shown persistent neurobehavioral changes and SRS that coincide with elevated levels of oxidative stress and neuroinflammation in the rat model of acute DFP intoxication. These data support the relevance of the rat DFP model to acute OP intoxication in humans. One caveat is the pretreatment with pyridostigmine used in model characterized here, which is likely not reflective of the majority of human victims of civilian mass casualties or suicide attempts involving OPs. We recently demonstrated that pyridostigmine pretreatment does not significantly alter the 24 h survival rate, scores of seizure behavior or inhibition of acetylcholinesterase activity in the brain (Bruun et al., 2019). Ongoing studies in our laboratory indicate that neuropathology, behavior, and SRS following acute DFP intoxication do not differ significantly between DFP animals pretreated with PB or not (unpublished data). This likely reflects the fact that PB does not cross the blood brain barrier to any appreciable extent (Lorke and Petroianu, 2019), and suggests that there is little influence of peripheral effects of acute DFP intoxication on outcomes in the brain.

An outstanding question not addressed in this study is whether the persistent neurologic effects of acute DFP intoxication are due to the chemical, acute SE or SRS. Also not addressed in this study is the causal relationship between DFP-induced neuroinflammation/oxidative stress and persistent neurobehavioral changes and SRS. Nonetheless, the data presented here suggest that evaluation of anti-oxidant and anti-neuroinflammatory agents for efficacy in protecting against the long-term neurologic sequelae of acute OP intoxication is warranted. Given the similarity in changes observed in the rat model of acute DFP intoxication to those observed in human and animal models of mesial temporal lobe epilepsy (Cavarsan et al., 2018; Janz et al., 2017; Nguyen et al., 2018), mechanistic and therapeutic testing studies in the DFP rat may be of translational value to this most common focal epilepsy that is often refractory to medication.

Funding

This work was supported by the National Institutes of Health CounterACT program [grant number NS079202], the National Institute of General Medical Sciences [grant number T32 GM099608], and the David and Dana Loury Foundation [predoctoral fellowship to M.G and B.A.H.]. This project used core facilities supported by the MIND Institute Intellectual and Developmental Disabilities Research Center (U54 HD079125). The sponsors were not involved in the study design, the collection, analysis and interpretation of data, the writing of the paper or in the decision to submit the work for publication.

Declaration of interest

None.

References

Ahsan, H., 2013. 3-Nitrotyrosine: a biomarker of nitrogen free radical species modified proteins in systemic autoimmunogenic conditions. Hum. Immunol. 74, 1392–1399.
Banks, C.N., Lein, P.J., 2012. A review of experimental evidence linking neurotoxic organophosphorus compounds and inflammation. Neurotoxicology 33, 575–584.
Bird, S.B., Gaspari, R.J., Dickson, E.W., 2003. Early death due to severe organophosphate poisoning is a centrally mediated process. Acad. Emerg. Med. 10, 295–298.
Brewer, K.L., Troendle, M.M., Pekman, L., Meggs, W.J., 2013. Naltrexone prevents delayed encephalopathy in rats poisoned with the sarin analogue diisopropylflurophosphate. Am. J. Emerg. Med. 31, 676–679.
Bruun, D.A., Guignet, M., Harvey, D.J., Lein, P.J., 2019. Pretreatment with pyridostigmine bromide has no effect on seizure behavior or 24 hour survival in the rat model of acute diisopropyl fluorophosphate intoxication. Neurotoxicology 73, 81–84 in press.
Cavarsan, C.F., Malheiros, J., Hamani, C., Najm, I., Covolan, L., 2018. Is mossy Fiber sprouting a potential therapeutic target for epilepsy? Front. Neurol. 9, 1023.
Chen, Y., 2012. Organophosphate-induced brain damage: mechanisms, neuropsychiatric and neurological consequences, and potential therapeutic strategies. Neurotoxicology 33, 391–400.
Collombet, J.M., 2011. Nerve agent intoxication: recent neuropathophysiological findings and subsequent impact on medical management prospects. Toxicol. Appl. Pharmacol. 255, 229–241.
Costa, L.G., 2006. Current issues in organophosphate toxicology. Clin. Chim. Acta 366, 1–13.
Coubard, S., Beracochea, D., Collombet, J.M., Philippin, J.N., Krazem, A., Liscia, P., et al., 2008. Long-term consequences of soman poisoning in mice: part 2. Emot. Behav. Behav. Brain Res. 191, 95–103.
Cowan, C.S.M., Richardson, R., 2018. A brief guide to studying fear in developing rodents: important considerations and common pitfalls. Curr. Protoc. Neurosci. 83, e44.
Damodaran, T.V., Abou-Donia, M.B., 2000. Alterations in levels of mRNAs coding for glial fibrillary acidic protein (GFAP) and vimentin genes in the central nervous system of hens treated with diisopropyl phosphorofluoridate (DFP). Neurochem. Res. 25, 809–816.
de Araujo, Furtado M., Lumley, L.A., Robison, C., Tong, L.C., Lichtenstein, S., Yourick, D.L., 2010. Spontaneous recurrent seizures after status epilepticus induced by soman in Sprague-Dawley rats. Epilepsia 51, 1503–1510.
de Araujo, Furtado M., Rossetti, F., Chanda, S., Yourick, D., 2012. Exposure to nerve agents: from status epilepticus to neuroinflammation, brain damage, neurogenesis and epilepsy. Neurotoxicology 33, 1476–1490.
Deshpande, L.S., Carter, D.S., Blair, R.E., DeLorenzo, R.J., 2010. Development of a prolonged calcium plateau in hippocampal neurons in rats surviving status epilepticus induced by the organophosphate diisopropylfluorophosphate. Toxicol. Sci. 116, 623–631.
Deshpande, L.S., Phillips, K., Huang, B., DeLorenzo, R.J., 2014. Chronic behavioral and cognitive deficits in a rat survival model of paraoxon toxicity. Neurotoxicology 44, 352–357.
Eddleston, M., Buckley, N.A., Eyer, P., Dawson, A.H., 2008. Management of acute organophosphorus pesticide poisoning. Lancet 371, 597–607.
Flannery, B.M., Bruun, D.A., Rowland, D.J., Banks, C.N., Austin, A.T., Kukis, D.L., et al., 2016. Persistent neuroinflammation and cognitive impairment in a rat model of acute diisopropylfluorophosphate intoxication. J. Neuroinflammation 13, 267.
Gao, J., Naughton, S.X., Wulff, H., Singh, V., Beck, W.D., Magrane, J., et al., 2016. Diisopropylfluorophosphate impairs the transport of membrane-bound organelles in rat cortical axons. J. Pharmacol. Exp. Ther. 356, 645–655.
Grauer, E., Chapman, S., Rabinovitz, I., Raveh, L., Weissman, B.A., Kadar, T., et al., 2008. Single whole-body exposure to sarin vapor in rats: long-term neuronal and behavioral deficits. Toxicol. Appl. Pharmacol. 227, 265–274.
Guignet, M., Lein, P.J., 2018. Organophosphates. In: Aschner, M., Costa, L.G. (Eds.), Advances in Neurotoxicology: Role of Inflammation in Environmental Neurotoxicity. Elsevier, Ltd., Oxford, UK, pp. 35–79.
Guilarte, T.R., 2019. TSPO in diverse CNS pathologies and psychiatric disease: a critical review and a way forward. Pharmacol. Ther. 194, 44–58.
Gunnell, D., Eddleston, M., Phillips, M.R., Konradsen, F., 2007. The global distribution of fatal pesticide self-poisoning: systematic review. BMC Public Health 7, 357.
Haley, N., 2018. Remarks at an Emergency UN Security Council Briefing on Chemical Weapons Use by Russia in the United Kingdom. United States Mission to the United Nations.
Hayden, K.M., Norton, M.C., Darcey, D., Ostbye, T., Zandi, P.P., Breitner, J.C., et al., 2010. Occupational exposure to pesticides increases the risk of incident AD: the Cache County study. Neurology 74, 1524–1530.
Heiss, D.R., Zehnder 2nd, D.W., Jett, D.A., Platoff Jr., G.E., Yeung, D.T., Brewer, B.N., 2016. Synthesis and storage stability of Diisopropylfluorophosphate. J. Chemother. 2016.
Hobson, B.A., Siso, S., Rowland, D.J., Harvey, D.J., Bruun, D.A., Garbow, J.R., et al., 2017. From the cover: MagneticResonance imaging reveals progressive brain injury in rats acutely intoxicated with Diisopropylfluorophosphate. Toxicol. Sci. 157, 342–353.
Hulse, E.J., Davies, J.O., Simpson, A.J., Sciuto, A.M., Eddleston, M., 2014. Respiratory complications of organophosphorus nerve agent and insecticide poisoning. Implications for respiratory and critical care. Am. J. Respir. Crit. Care Med. 190, 1342–1354.
Janz, P., Schwaderlapp, N., Heining, K., Haussler, U., Korvink, J.G., von Elverfeldt, D., et al., 2017. Early tissue damage and microstructural reorganization predict disease severity in experimental epilepsy. Elife 6.

Jett, D.A., Spriggs, S.M., 2018. Translational research on chemical nerve agents. Neurobiol. Dis. S0969-9961 (18), 30751–30754. https://doi.org/10.1016/j.nbd.2018.11.020. [Epub ahead of print].
Kim, Y.B., Hur, G.H., Shin, S., Sok, D.E., Kang, J.K., Lee, Y.S., 1999. Organophosphate-induced brain injuries: delayed apoptosis mediated by nitric oxide. Environ. Toxicol. Pharmacol. 7, 147–152.
Kruger, L., Saporta, S., Swanson, L.W., 1995. Photographic Atlas of the Rat Brain: The Cell and Fiber Architecture Illustrated in Three Planes with Stereotaxic Coordinates. Cambridge University Press, Cambridge.
Kuruba, R., Wu, X., Reddy, D.S., 2018. Benzodiazepine-refractory status epilepticus, neuroinflammation, and interneuron neurodegeneration after acute organophosphate intoxication. Biochim. Biophys. Acta Mol. basis Dis. 1864, 2845–2858.
Levin, H.S., Rodnitzky, R.L., Mick, D.L., 1976. Anxiety associated with exposure to organophosphate compounds. Arch. Gen. Psychiatry 33, 225–228.
Li, Y., Lein, P.J., Liu, C., Bruun, D.A., Tewolde, T., Ford, G., et al., 2011. Spatiotemporal pattern of neuronal injury induced by DFP in rats: a model for delayed neuronal cell death following acute OP intoxication. Toxicol. Appl. Pharmacol. 253, 261–269.
Li, Y., Lein, P.J., Ford, G.D., Liu, C., Stovall, K.C., White, T.E., et al., 2015. Neuregulin-1 inhibits neuroinflammatory responses in a rat model of organophosphate-nerve agent-induced delayed neuronal injury. J. Neuroinflammation 12, 64.
Liang, L.P., Pearson-Smith, J.N., Huang, J., McElroy, P., Day, B.J., Patel, M., 2018. Neuroprotective effects of AEOL10150 in a rat organophosphate model. Toxicol. Sci. 162, 611–621.
Liu, C., Li, Y., Lein, P.J., Ford, B.D., 2012. Spatiotemporal patterns of GFAP upregulation in rat brain following acute intoxication with diisopropylfluorophosphate (DFP). Curr. Neurobiol. 3, 90–97.
Lopez-Crespo, G.A., Flores, P., Sanchez-Santed, F., Sanchez-Amate, M.C., 2009. Acute high dose of chlorpyrifos alters performance of rats in the elevated plus-maze and the elevated T-maze. Neurotoxicology 30, 1025–1029.
Lorke, D.E., Petroianu, G.A., 2019. Reversible cholinesterase inhibitors as pretreatment for exposure to organophosphates. A review. J. Appl. Toxicol. 39, 101–116.
Lugrin, J., Rosenblatt-Velin, N., Parapanov, R., Liaudet, L., 2014. The role of oxidative stress during inflammatory processes. Biol. Chem. 395, 203–230.
Mew, E.J., Padmanathan, P., Konradsen, F., Eddleston, M., Chang, S.S., Phillips, M.R., et al., 2017. The global burden of fatal self-poisoning with pesticides 2006-15: systematic review. J. Affect. Disord. 219, 93–104.
Miyaki, K., Nishiwaki, Y., Maekawa, K., Ogawa, Y., Asukai, N., Yoshimura, K., et al., 2005. Effects of sarin on the nervous system of subway workers seven years after the Tokyo subway sarin attack. J. Occup. Health 47, 299–304.
Nguyen, D.L., Wimberley, C., Truillet, C., Jego, B., Caille, F., Pottier, G., et al., 2018. Longitudinal positron emission tomography imaging of glial cell activation in a mouse model of mesial temporal lobe epilepsy: toward identification of optimal treatment windows. Epilepsia 59, 1234–1244.
Nishiwaki, Y., Maekawa, K., Ogawa, Y., Asukai, N., Minami, M., Omae, K., et al., 2001. Effects of sarin on the nervous system in rescue team staff members and police officers 3 years after the Tokyo subway sarin attack. Environ. Health Perspect. 109, 1169–1173.
Okumura, T., Hisaoka, T., Naito, T., Isonuma, H., Okumura, S., Miura, K., et al., 2005. Acute and chronic effects of sarin exposure from the Tokyo subway incident. Environ. Toxicol. Pharmacol. 19, 447–450.
OPCW, 2017. Report on the Use of a Chemical Weapon in the Death of a DPRK National. Organisation for the Prohibition of Chemical Weapons.
Pearson, J.N., Patel, M., 2016. The role of oxidative stress in organophosphate and nerve agent toxicity. Ann. N. Y. Acad. Sci. 1378, 17–24.
Pereira, E.F., Aracava, Y., DeTolla Jr., L.J., Beecham, E.J., Basinger Jr., G.W., Wakayama, E.J., et al., 2014. Animal models that best reproduce the clinical manifestations of human intoxication with organophosphorus compounds. J. Pharmacol. Exp. Ther. 350, 313–321.
Pessah, I.N., Rogawski, M.A., Tancredi, D.J., Wulff, H., Zolkowska, D., Bruun, D.A., et al., 2016. Models to identify treatments for the acute and persistent effects of seizure-inducing chemical threat agents. Ann. N. Y. Acad. Sci. 1378, 124–136.
Pope, C.N., 1999. Organophosphorus pesticides: do they all have the same mechanism of toxicity? J. Toxicol. Environ. Health B Crit. Rev. 2, 161–181.
Pouliot, W., Bealer, S.L., Roach, B., Dudek, F.E., 2016. A rodent model of human organophosphate exposure producing status epilepticus and neuropathology. Neurotoxicology 56, 196–203.
Prager, E.M., Pidoplichko, V.I., Aroniadou-Anderjaska, V., Apland, J.P., Braga, M.F., 2014. Pathophysiological mechanisms underlying increased anxiety after soman exposure: reduced GABAergic inhibition in the basolateral amygdala. Neurotoxicology 44, 335–343.
Raffaele, K., Hughey, D., Wenk, G., Olton, D., Modrow, H., McDonough, J., 1987. Long-term behavioral changes in rats following organophosphonate exposure. Pharmacol. Biochem. Behav. 27, 407–412.
Rajbhandari, A.K., Gonzalez, S.T., Fanselow, M.S., 2018 Oct 13. Stress-enhanced fear learning, a robust rodent model of post-traumatic stress disorder. J. Vis. Exp. 140. https://doi.org/10.3791/58306.
Rojas, A., Ganesh, T., Lelutiu, N., Gueorguieva, P., Dingledine, R., 2015. Inhibition of the prostaglandin EP2 receptor is neuroprotective and accelerates functional recovery in a rat model of organophosphorus induced status epilepticus. Neuropharmacology 93, 15–27.
Rojas, A., Ganesh, T., Manji, Z., O'Neill, T., Dingledine, R., 2016. Inhibition of the prostaglandin E2 receptor EP2 prevents status epilepticus-induced deficits in the novel object recognition task in rats. Neuropharmacology 110, 419–430.
Rosenbaum, C., Bird, S.B., 2010. Non-muscarinic therapeutic targets for acute organophosphorus poisoning. J. Med. Toxicol. 6, 408–412.
Shrot, S., Ramaty, E., Biala, Y., Bar-Klein, G., Daninos, M., Kamintsky, L., et al., 2014. Prevention of organophosphate-induced chronic epilepsy by early benzodiazepine treatment. Toxicology 323, 19–25.
Siso, S., Hobson, B.A., Harvey, D.J., Bruun, D.A., Rowland, D.J., Garbow, J.R., et al., 2017. Editor's highlight: spatiotemporal progression and remission of lesions in the rat brain following acute intoxication with Diisopropylfluorophosphate. Toxicol. Sci. 157, 330–341.
Sogorb, M., Estevez, J., Vilanova, E., 2015. Toxicokinetics and Toxicodynamics of DFP. In: Gupta, R.C. (Ed.), Handbook of Toxicology of Chemical Warfare Agents, 2nd ed. Elsevier, USA.
UN, 2017. Report of the Independent International Commission of Inquiry on the Syrian Arab Republic United Nations General Assembly: Human Rights Council.
Vanova, N., Pejchal, J., Herman, D., Dlabkova, A., Jun, D., 2018. Oxidative stress in organophosphate poisoning: role of standard antidotal therapy. J. Appl. Toxicol. 38, 1058–1070.
Vogel, L., 2013. WHO releases guidelines for treating chemical warfare victims after possible Syria attacks. CMAJ 185, E665-E.
Waheed, S., Sabeen, A., Ullah, Khan N., 2014. New onset refractory status epilepticus as an unusual presentation of a suspected organophosphate poisoning. Case Rep. Emerg. Med. 2014, 676358.
Wilkinson, B.L., Landreth, G.E., 2006. The microglial NADPH oxidase complex as a source of oxidative stress in Alzheimer's disease. J. Neuroinflammation 3, 30.
Wright, L.K., Liu, J., Nallapaneni, A., Pope, C.N., 2010. Behavioral sequelae following acute diisopropylfluorophosphate intoxication in rats: comparative effects of atropine and cannabinomimetics. Neurotoxicol. Teratol. 32, 329–335.
Wu, X., Kuruba, R., Reddy, D.S., 2018. Midazolam-resistant seizures and brain injury after acute intoxication of Diisopropylfluorophosphate, an organophosphate pesticide and surrogate for nerve agents. J. Pharmacol. Exp. Ther. 367, 302–321.
Yokoyama, K., Araki, S., Murata, K., Nishikitani, M., Okumura, T., Ishimatsu, S., et al., 1998. Chronic neurobehavioral effects of Tokyo subway sarin poisoning in relation to posttraumatic stress disorder. Arch. Environ. Health 53, 249–256.
Zaja-Milatovic, S., Gupta, R.C., Aschner, M., Milatovic, D., 2009. Protection of DFP-induced oxidative damage and neurodegeneration by antioxidants and NMDA receptor antagonist. Toxicol. Appl. Pharmacol. 240, 124–131.